Studies on the functional domains involved in hepatitis B virus early infection machinery

B 型肝炎ウイルス初期感染機構を担う機能性ドメインの解析

Department of Biomolecular Science and Reaction
The Institute of Scientific and Industrial Research, Osaka university
大阪大学産業科学研究所　生体分子反応科学研究分野

Graduate School of Frontier Biosciences, Osaka University
大阪大学大学院生命機能研究科　生命機能専攻

Qiushi LIU
刘　秋実

March, 2019

研究の背景、目的、位置づけ、意義と新規性

【背景】B 型肝炎ウイルス（HBV）は血液や体液により伝播し、ヒト肝臓組織に特異的かつ高効率で感染し、肝炎、肝硬変、肝癌等の重篤な肝疾患を引き起こすウイルスである。世界中の約 3 億人が HBV に感染し、深刻な社会問題になっている。ワクチン接種により HBV 伝播をある程度抑えることに成功しているが、HBV 生活環、特に初期感染機構（具体的には、①HBV 外皮 L タンパク質とヒト肝臓細胞の吸着、②エンドサイトーシス誘導、③HBV 膜とエンドソーム膜の融合、④HBV 内部（コアとゲノム）の脱殻）が分子レベルで未解明なため、HBV 治療薬の開発が遅れている。近年、ヒト肝臓細胞に、低親和性 HBV 受容体の「ヘパラン硫酸プロテオグリカン（HSPG）」と高親和性 HBV 受容体の「Na 胆汁酸トランスポーター（NTCP）」の存在が明らかにされたが、HBV 初期感染機構における作用機作は不明である。

【目的】これまでに私の所属する研究室では、ヒト肝臓細胞表層において HBV は NTCP ではなく HSPG とのみ相互作用すること、*in vitro* において HBV 外皮 L タンパク質の N 末端部分（9-24）が酸性依存性膜融合ドメインとして機能することを見出している。しかし、HBV 初期感染の第 1 段階を支える「HBV 外皮 L タンパク質内の HSPG 相互作用部位」が不明であった。また、HBV 初期感染の第 3 及び第 4 段階を支える「上記膜融合ドメインの重要アミノ酸残基」も不明であった。本研究では、これらの HBV の初期感染機構を支える重要な部位や残基を明らかにすることを目的としている。

【位置づけ】本研究は、ウイルス学における HBV の初期感染機構解明に関する。また、HBV の初期感染機構を搭載した、薬物送達（Drug Delivery System, DDS）用ナノキャリアの開発に関する。

【意義】本研究の成果は、HBV 治療薬の全く新しい創薬ポイントを提供する。また、HBV は生体内において肝臓特異的に感染し、HBV ゲノムを高効率で送達

させ感染成立する。これは、HBV はウイルスの進化過程で最適化された天然 DDS ナノキャリアであり、既存の人工 DDS ナノキャリアでは達成困難な性能を有している。本研究の成果は、その高度な性能を支える HBV 初期感染機構を分子レベルで明らかにしたものであり、ウイルス由来でありながら人工 DDS ナノキャリアである「HBV 外皮 L タンパク質のみで構成されたバイオナノカプセル」の実用化に大きく貢献する。

【新規性】本研究により、HBV 外皮 L タンパク質の N 末端部分（30-42）が、低親和性 HBV 受容体 HSPG と結合することを初めて見出した。この相互作用が、HBV が最初にヒト肝臓細胞表層に接着するのに必須であると考えられる。また、同（30-42）ペプチドは、既報の多くの HSPG 及びヘパラン硫酸結合ドメインと異なり、ヒト肝臓細胞由来 HSPG に高い親和性を有していることから、ヒト肝臓特異的 DDS ナノキャリアの標的分子として有効であることも判明した。

次に、既報の多くの膜融合ドメインが、その正電荷により膜表面（負電荷）と相互作用することで駆動するのに対し、HBV 外皮 L タンパク質の膜融合ドメイン（9-24）は疎水性クラスターが膜と相互作用することで駆動することを初めて見出した。また、同ドメイン内の Asp 残基が酸性 pH 条件下で疎水的となることで、細胞内エンドソームにおいて膜融合活性が高まり、エンドソーム膜と HBV 膜の融合を引き起こし、最終的に HBV の脱殻を誘導するモデルを提唱した。

Abstract

Hepatitis B virus (HBV) is an approximately 42-nm envelope DNA virus that can infect human hepatic cells specifically. While heparan sulfate proteoglycan (HSPG) and sodium taurocholate co-transporting polypeptide (NTCP) were recently identified as low-affinity and high-affinity HBV receptor, respectively, the early infection machinery including cell attachment, cell entry, endosomal escape, and uncoating has not been fully elucidated on the molecular basis. In this thesis, I identified a novel HSPG-interacting domain in the pre-S1 region, pre-S1(30-42). The domain preferentially attaches with human hepatic cells, which is indispensable for the cell attachment of HBV. Furthermore, I analyzed the low pH-dependent fusogenic domain in the pre-S1 region, pre-S1(9-24), by using mutated peptides and an endosomal membrane model. Unlike conventional fusogenic domains which require positively charged residues, the fusogenic activity of pre-S1(9-24) is dependent on the hydrophobicity of whole structure. Taken together, HBV could interact with HSPG on human hepatic cells via pre-S1(30-42), enter cells by endocytosis, transfer to NTCP, and then initiate endosomal escape (including subsequent uncoating) through the fusion with endosomal membrane by pre-S1(9-24) under acidic conditions in late endosomes. On the other hand, the nanoparticles consisting of HBV envelope L protein exclusively (i.e., bio-nanocapsules (BNCs)) have been developed as an efficient drug delivery system (DDS) nanocarrier equipped with the HBV early infection machinery. Due to complicated CMC (chemistry, manufacturing, and controls) caused by the nature of biologics, the application of BNCs has been severely restricted. The results described in this thesis would shed light on the molecular basis of HBV early infection machinery, and thereby could contribute to the development of HBV-mimicking

DDS nanocarriers with simple CMC by reconstituting the machinery on the conventional chemical DDS nanocarriers.

Index

Chapter I

General Introduction

Hepatitis B virus (HBV) is an approximately 42-nm envelope DNA virus which could infect human hepatic cells specifically and efficiently [1]. HBV causes severe liver-related diseases, such as hepatitis, cirrhosis, and liver cancer. Three types of envelope proteins were found on the surface of HBV virion; S protein (S region), M protein (pre-S2 + S region), and L protein (pre-S1 + pre-S2 + S region), of which the stoichiometric ratio in HBV virion is approximately 4:1:1 [2] (Fig. 1). While HBV was discovered about 40 years ago, HB vaccine is the only way for preventing the spread of HBV infection. It

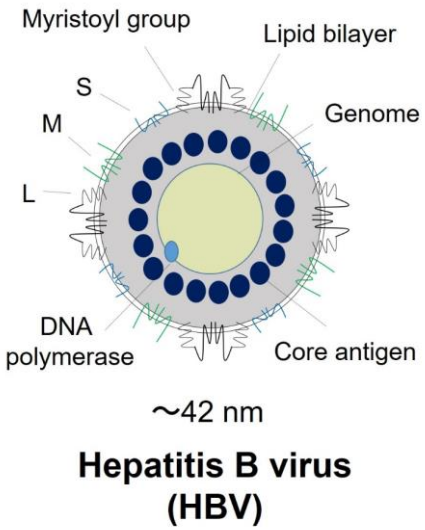

Fig. 1 The structure of hepatitis B virus.

has so far been nearly impossible to eliminate virions from HB patients. For developing effective anti-HBV drugs, it is important to elucidate the infection and replication machinery of HBV on the molecular basis.

Many natural nanoparticles including viruses [3, 4], exosomes [5] were found to utilize the cell-surface HSPG as an endocytosis receptor. Concerning about the early

infection machinery consisting of cell attachment, cell entry, endosomal escape, and uncoating (Fig. 2), HBV interacts primarily with heparan sulfate proteoglycan (HSPG) on cell surface, especially highly sulfated glycosaminoglycans (GAGs), which mainly determines the hepatotropism of HBV [6]. As for the HSPG-interacting domain of HBV, while various regions have been proposed [6-9], it has been controversial which residues play crucial role. Highly conserved residues (Gly-282, Pro-283, Cys-284, Arg-285, Cys-

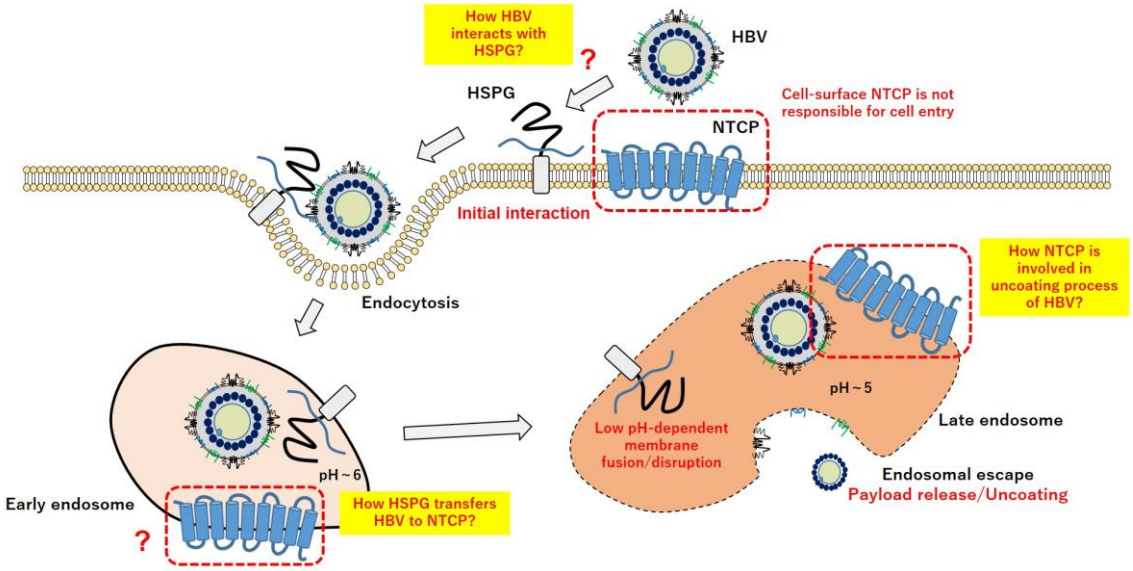

Fig. 2 The early infection machinery of hepatitis B virus.

287, and Lys-312) in the antigenic loop of S region are likely responsible for HSPG interaction [6-8] (Fig. 3). Meanwhile, the pre-S1 region also binds to heparin *in vitro*. Hence, it has remained unclear how these interactions are involved in the early HBV infection machinery [9]. Recently, two types of HBV virion were found, of which the pre-S region is hidden and exposed in its envelope membrane (N-type HBV and B-type HBV, respectively) [10]. When the pre-S region hidden in its interior cavity, the N-type HBV could not bind to HSPG and primary human hepatocytes, while the B-type HBV could. This result confirmed that the conformational change of HBV triggers the deployment of

pre-S1 region outwardly and then enables the interaction of pre-S1 region with HSPG, leading to the cell entry of HBV by clathrin-mediated endocytosis or micropinocytosis [11, 12] (Fig. 2). Recently, HBV was indicated to interact with a high affinity functional HBV receptor, sodium taurocholate-cotransporting polypeptide (NTCP), via the N-terminal myristoylated pre-S1(2-47) region [13]. However, our group demonstrated that cell-surface NTCP is not involved in the cell entry of HBV and proposed that endosomal NTCP is involved in the endosomal escape and uncoating step of HBV [14, 15] (*see* below). Instead, highly sulfated HSPG on cell surface was shown to be responsible for the HBV cell entry [14]. In Chapter III, I delineated the essential region for HSPG interaction in pre-S1 region for clarifying the cell attachment and entry of HBV on the molecular basis.

Since HBV is an enveloped virus (Fig. 1), core particle containing HBV genome should be released from endosomes to cytoplasm after the fusion with endosomal membrane (*i.e.*, endosomal escape) for establishing the HBV infection. So far, two fusogenic domains have been identified at pre-S2(149-160) and S(164-186) [16, 17], the

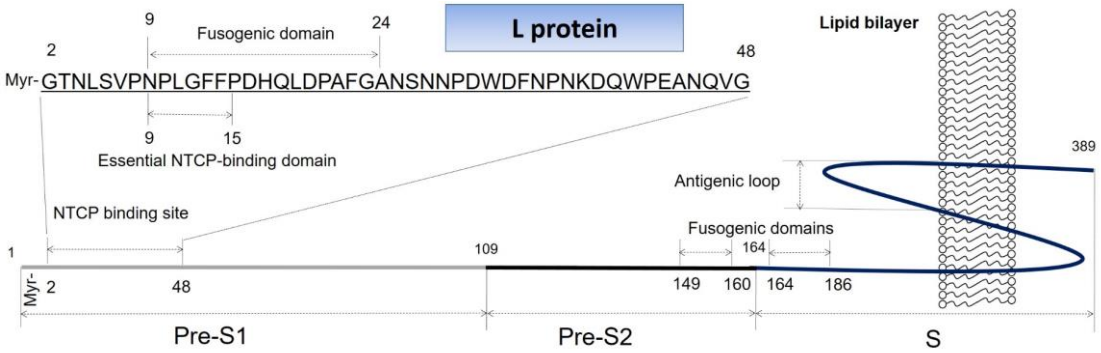

Fig. 3 The functional domains in L protein.

former is pH-independent and the latter is low pH-dependent (Fig. 3). However, trypsinized HB particle, containing S and M proteins exclusively, showed no fusogenic

activity in the *in vitro* liposomal fusion assay [18], suggesting other fusogenic domain in pre-S1 region is crucial for the endosomal escape of HBV. Recently, our group identified a low pH-dependent fusogenic domain in the N-terminal pre-S1 region, named as pre-S1(9-24) [18], which includes the essential NTCP-binding domain pre-S1(9-15) [19]. It was therefore postulated that the interaction of endosomal NTCP with the myristoyl residue and pre-S1(9-15) under acidic condition enhances the fusogenic activity of pre-S1(9-24) for undergoing the endosomal escape and uncoating of HBV (Fig. 2). In Chapter II, I investigated which residues in pre-S1(9-24) are responsible for the interaction with endosomal membrane. In future, by combining with the results of NTCP studies, it will be elucidated how NTCP and pre-S1(9-24) synergistically contributes to the uncoating process of HBV. This result would shed light on the mechanism how HBV interacts with HSPG, enters cells, and transfers from HSPG to NTCP.

References

1. P. Tiollais, C. Pourcel, A. Dejean, The hepatitis B virus, *Nature*, 1985, 317, 489-495.
2. V. Bruss, Hepatitis B virus morphogenesis, *World Journal of Gastroenterology*, 2007, 13, 65-73.
3. C.E. Thomas, A. Ehrhardt, M.A. Kay, Progress and problems with the use of viral vectors for gene therapy, *Nature Reviews Genetics*, 2003, 4, 346-358.
4. P.D. Robbins, S.C. Ghivizzani, Viral vectors for gene therapy, *Pharmacology & Therapeutics*, 1998, 80, 35-47.
5. Helena C. Christianson, Katrin J. Svensson, Toin H. van Kuppevelt, Jin-Ping Li, and Mattias Belting, Cancer cell exosomes depend on cell-surface heparin sulfate proteoglycans for their internalization and functional activity, *Proceedings of the*

National Academy of Sciences of the United States of America, 2013, 110, 17380-17385.

6. J. Salisse, C. Sureau, A function essential to viral entry underlies the hepatitis B virus "a" determinant, *Journal of virology*, 2009, 83, 9321-9328.
7. C. Sureau, J. Salisse, A conformational heparan sulfate binding site essential to infectivity overlaps with the conserved hepatitis B virus a-determinant, *Hepatology*, 2013, 57, 985-994.
8. G. Abou-Jaoudé, C. Sureau, Entry of hepatitis delta virus requires the conserved cysteine residues of the hepatitis B virus envelope protein antigenic loop and is blocked by inhibitors of thiol-disulfide exchange, *Journal of Virology*, 2007, 81, 13057-13066.
9. C.M. Leistner, S. Gruen-Bernhard, D. Glebe, Role of glycosaminoglycans for binding and infection of hepatitis B virus, *Cellular Microbiology*, 2008, 10, 122-133.
10. S. Seitz, C. Iancu, T. Volz, W. Mier, M. Dandri, S. Urban, R. Bartenschlager, A slow maturation process renders hepatitis B virus infectious, *Cell Host & Microbe*, 2016, 20, 25-35.
11. M. Yamada, A. Oeda, J. Jung, M. Iijima, N. Yoshimoto, T. Niimi, S.Y. Jeong, E.K. Choi, K. Tanizawa, S. Kuroda, Hepatitis B virus envelope L protein-derived bio-nanocapsules: mechanisms of cellular attachment and entry into human hepatic cells, *Journal of Controlled Release*, 2012, 160, 322-329.
12. H.C. Huang, C.C. Chen, W.C. Chang, M.H. Tao, C. Huang, Entry of hepatitis B virus into immortalized human primary hepatocytes by clathrin-dependent endocytosis, *Journal of Virology*, 2012, 86, 9443-9453.
13. H. Yan, G. Zhong, G. Xu, W. He, Z. Jing, Z. Gao, Y. Huang, Y. Qi, B. Peng, H. Wang,

L. Fu, M. Song, P. Chen, W. Gao, B. Ren, Y. Sun, T. Cai, X. Feng, J. Sui, W. Li, Sodium taurocholate cotransporting polypeptide is a functional receptor for human hepatitis B and D virus, *eLife*, 2012, 1, e00049.

14. M. Somiya, Q. Liu, N. Yoshimoto, M. Iijima, K. Tatematsu, T. Nakai, T. Okajima, K. Kuroki, K. Ueda, S. Kuroda, Cellular uptake of hepatitis B virus envelope L particles is independent of sodium taurocholate cotransporting polypeptide, but dependent on heparan sulfate proteoglycan, *Virology*, 2016, 497, 23-32.
15. M. Somiya, S. Kuroda, Development of a virus-mimicking nanocarrier for drug delivery systems: The bio-nanocapsule, *Advanced Drug Delivery Reviews*, 2015, 95, 77-89.
16. S. Oess, E. Hildt, Novel cell permeable motif derived from the PreS2-domain of Hepatitis-B virus surface antigens, *Gene Therapy*, 2000, 7, 750-758.
17. I. Rodríguez-Crespo, J. Gómez-Gutiérrez, M. Nieto, D.L. Peterson, F. Gavilanes, Prediction of a putative fusion peptide in the S protein of hepatitis B virus, *Journal of General Virology*, 1994, 75, 637-639.
18. M. Somiya, Y. Sasaki, T. Matsuzaki, Q. Liu, M. Iijima, N. Yoshimoto, T. Niimi, A.D. Maturana, S. Kuroda, Intracellular trafficking of bio-nanocapsule-liposome complex: Identification of fusogenic activity in the pre-S1 region of hepatitis B virus surface antigen L protein, *Journal of Controlled Release*, 2015, 212, 10-18.
19. S. Urban, R. Bartenschlager, R. Kubitz, F. Zoulim, Strategies to inhibit entry of HBV and HDV into hepatocytes, *Gastroenterology*, 2014, 147, 48-64.

Chapter II

Mutational Analysis of Hepatitis B Virus Pre-S1 (9-24) Fusogenic Peptide

2.1. Introduction

Enveloped viruses require fusion with the plasma membrane or endosomal membrane for their uncoating process, thereby allowing them to release the internal components (*e.g.*, genome, capsids, and polymerase) to the cytoplasm [1, 2]. In general, fusion protein, a part of the envelope proteins, possesses fusion peptides or fusion loops forming a hydrophobic membrane at proximal regions at the junction between the ectodomain and membrane anchor. When the fusion of two membranes proceeds by the formation of a dehydration interface, and a hemifusion stalk is formed followed by a fusion pore, either the fusion peptides or fusion loops could be deposited onto fusion proteins by priming events (*e.g.*, proteolytic cleavage, receptor attachment, low pH environment), leading to a change in the secondary structure caused by the acidic conditions in endosomes. After insertion into the endosomal membrane, a dehydration interface can be formed, which then enhances the membrane perturbation to form the hemifusion stalk [1]. For example, the fusion peptide of influenza virus hemagglutinin protein was shown to slightly increase α-helicity by the protonation onto residues E15 and D19 in endosomes, leading to the fusion between the viral membrane and endosomal membrane [3]. Hepatitis B virus (HBV) is also an enveloped virus, consisting of small [S, 226 amino acid residues (aa)], middle (M; pre-S2+S, 281 aa), and large [L; pre-S1+pre-S2+S, 389 aa (serotype, ayw) or 400 aa (serotype adr)] envelope proteins [4]. HBV is considered to attach specifically to human hepatic cells, enter the cells by receptor-

mediated endocytosis, and then execute subsequent membrane fusion for the transfer of its genome and accessory proteins to the cytoplasm (*i.e.*, uncoating process) [5]. The following fusogenic domains were independently identified in L protein: the C-terminal half of the pre-S2 region [pH-independent, from 149 to 160 aa of L protein (ayw)] [6], the N-terminal part of the S region [low pH-dependent, 164–186 aa of L protein (ayw)] [7, 8], and the whole pre-S1 region (low pH-dependent) [9]; however, it has thus far remained controversial as to which domains in the L envelope protein are responsible for the uncoating process of HBV in endosomes. In 2003, HBV envelope L protein particles synthesized in *Saccharomyces cerevisiae* were found to infect human hepatic cells *in vitro* and *in vivo* by HBV-derived infection machinery [10-12]. Our group therefore designated an HBV bio-mimicking nanoparticle as a bio-nanocapsule (BNC). Recently, using a lipid mixing assay with liposomes (LPs) labeled with fluorescence resonance energy transfer (FRET) pairs, the membrane portion of the BNC was found to strongly fuse with LPs at low pH, indicating that L protein harbors functional low pH-dependent fusogenic activity. When the BNC was digested by trypsin to remove the whole pre-S1 region and N-terminal half of the pre-S2 region, but to retain the former two fusogenic domains (see above), the trypsinized BNC was found to lose its fusogenic activity completely [13], strongly suggesting that the pre-S1+pre-S2 regions are necessary for HBV membrane fusion. Finally, by using LPs displaying the pre-S1-derived peptides (20 aa each), our group identified that a low pH-dependent fusogenic domain resides in the N-terminal part of the pre-S1 region (NPLGFFPDHQLDPAFG, aa 9–24 of the L protein). Moreover, it was demonstrated that the BNC could not only fuse with target LPs but also disrupt its own membrane (payload release) and target LPs (membrane disruption) [13]. Since HBV displays the pre-S1+pre-S2 region outwardly as in the BNC, this suggests that the pre-S1

(9-24) peptide may play a pivotal role in the HBV uncoating process, as well as in the endosomal escape of the BNC's payload. In this study, I examined whether the pre-S1 (9-24) peptide itself possesses sufficient activity not only for membrane fusion but also for membrane disruption by using target LPs (a model of the endosomal membrane) containing a fluorophore and its quencher. By delineating the crucial aa for these activities by using mutated pre-S1 (9-24) peptides, I propose the mechanism for how the fusogenic peptide interacts with the membrane.

2.2. Experimental Procedures

2.2.1. Probe LPs for the lipid mixing assay

Dipalmitoylphosphatidylcholine (DPPC; NOF, Tokyo, Japan), dipalmitoylphosphatidylethanolamine (DPPE, NOF), dipalmitoylphosphatidylglycerol sodium salt (DPPG-Na, NOF), cholesterol (Nacalai Tesque, Kyoto, Japan), *N*-(7-nitrobenz-2-oxa-1,3- diazol-4-yl)-1,2-dihexadecanoyl-*sn*-glycero-3-phosphoethanolamine (NBD-PE; Life Technologies, Carlsbad, CA, USA), and lissamine rhodamine B 1,2-dihexadecanoyl-*sn*-glycero- 3-phosphoethanolamine, triethylammonium salt (Rh-DHPE; Life Technologies) were mixed at a molar ratio of 15:9:30:40:4:2, dissolved in a chloroform/methanol (2:1, v/v) mixture, and then evaporated at 37 ℃ using a rotary evaporator to form a thin hemispherical lipid film. NBD-derived fluorescence was designed to be quenched by the FRET effect. After hydrating the film with phosphate-buffered saline (PBS) at 60 ℃, the mixture was sonicated using an Astrason ultrasonic disruptor (Misonix, Farmingdale, NY, USA) for 15 min to obtain probe LPs of ~100 nm. The size of the LPs was measured in PBS at 25 ℃ using dynamic light scattering (Zetasizer Nano ZS; Malvern, Worcestershire, UK).

Lipid concentration was estimated from the cholesterol content, which was determined by a Cholesterol E-Test Wako kit (Wako, Osaka, Japan).

2.2.2. Peptide-displaying LPs

DPPC, cholesterol, and *N*-(3-maleimide-1-oxopropyl)-L-α-phosphatidylethanolamine, dioleoyl (NOF) were dissolved in ethanol at a molar ratio of 55:40:5, instilled into Tris-HCl (pH 8.0) buffer with gentle stirring at room temperature, and then subjected to a Sephadex G-25 gel filtration column (GE Healthcare, Buckinghamshire, UK) equilibrated with PBS. The LPs were incubated with synthetic peptides (purity, >95%; with a C-/N-terminal Cys modification; SCRUM Inc., Tokyo, Japan; *see* Table 1) at room temperature for 2 h to allow for a maleimide-thiol coupling reaction, maintained at 4 ℃ for 24 h, and then subjected to a Sephadex G-25 gel filtration column to remove the free peptides.

2.2.3. Lipid mixing assay

The probe LPs (NBD- and Rh-labeled, 10 μg) were pre-warmed in citrate buffer (pH 7.4, 9 mM citric acid, 91 mM Na_2HPO_4) or low-pH citrate buffer (pH 4.5, 56 mM citric acid, 44 mM Na_2HPO_4) at 37°C for 30 min. After the incubation with 20 μM of free peptides or 60 μg of 20 μM peptide-displaying LPs at 37 ℃ for 30 min, the NBD-derived fluorescence (excitation at 470 nm, emission at 540 nm) was measured on a Varioskan multiplate spectrophotometer (Thermo, Waltham, MA, USA). Triton X-100 was added at 1.0% (v/v) to quench the FRET effect. The percentage of NBD-derived fluorescence was calculated as follows: $\%F = (F_{NBD} - F_0)/(F_{100} - F_0)$, where F_0 is the initial NBD-derived fluorescence before the addition of samples, F_{NBD} is the NBD-derived

fluorescence after 30-min incubation with each sample, and F_{100} is the NBD-derived fluorescence after addition of Triton X-100.

2.2.4. Pyranine leakage assay

As described in Section 2.1, the mixture of DPPC, DPPE, DPPG-Na, and cholesterol at a molar ratio of 15:15:30:40 was allowed to form a thin hemispherical lipid film. By hydrating with PBS containing 35 mM pyranine (fluorophore; Sigma-Aldrich, St. Louis, MO, USA) and 50 mM *p*-xylene-bis (*N*-pyridinium bromide) (DPX, quencher; Sigma-Aldrich) at 60 ℃, the mixture was sonicated to obtain ~100-nm LPs, and then subjected to a Sephadex G-25 gel filtration column to remove free pyranine and free DPX. The LPs (containing pyranine and DPX, 4 μg) were pre-warmed in citric acid buffer at pH 7.4 or pH 4.5 at 37°C for 30 min. After incubation with 20 μM of free peptides or 60 μg peptide-displaying LPs at 37 ℃ for 30 min, the amount of leaked pyranine was determined by the pyranine-derived fluorescence (excitation at 416 nm, emission at 512 nm). Triton X-100 was added at 1.0% (v/v) to release pyranine from the LPs. The percentage of leaked pyranine was calculated as follows: pyranine leakage (%) = $(F_{pyranine} - F_0)/(F_{100} - F_0)$, where F_0 is the initial pyranine-derived fluorescence, $F_{pyranine}$ is the pyranine-derived fluorescence after 30-min incubation with each sample, and F_{100} is the pyranine-derived fluorescence after the addition of Triton X-100.

2.2.5. Circular dichroism (CD)

The CD spectra were obtained with 50 μM peptide in phosphate buffer (pH 7.4; 2 mM KH_2PO_4, 8 mM Na_2HPO_4) or low-pH phosphate buffer (pH 5.3; 97.5 mM KH_2PO_4, 2.5 mM Na_2HPO_4) at 25 ℃ on a JASCO J-725 CD spectropolarimeter (Tokyo, Japan)

using a 10-mm cell or a 1-mm cell [for the measurement with 2,2,2-trifluoroethanol (TFE)]. To examine the effect of the LPs, LPs containing DPPC, DPPE, DPPG-Na, and cholesterol at a molar ratio of 15:15:30:40 (*see* section 2.1) were added at 12.5 μM. Five scans at 0.5-nm resolution were averaged for each spectrum.

2.3. Results

2.3.1. Fusogenic and membrane disruption activity of the pre-S1 (9-24) peptide

The BNC showed membrane fusion, membrane disruption, and payload release activity in a low pH-dependent manner. Furthermore, low pH-dependent fusogenic activity was identified in the pre-S1 (9-24) region of the BNC by a lipid mixing assay [13]. When pre-S1 (9-24) peptide [wild type (WT) sequence]-displaying LPs were mixed with probe LPs labeled with NBD and Rh (FRET pair), the NBD-derived fluorescence was significantly enhanced by the shift from pH 7.4 to pH 4.5 (Fig. 4A).

The fusogenic activity of the peptide was changed from 5.9 ± 0.6% (mean ± SD, N = 3) to 28.1 ± 1.7% (mean ± SD, N = 3). Under the same condition, the free pre-S1 (9-24) peptide showed no fusogenic activity even at pH 4.5, indicating that the membrane anchoring is indispensable for the activity of the peptide. Moreover, low pH-dependent membrane disruption activity was also identified in BNC by a pyranine leakage assay [13]. The pre-S1 (9-24) peptide-displaying LPs exhibited the same activity in a low pH-dependent manner (Fig. 4B), which was comparable to that of the LPs displaying human immunodeficiency virus tat-derived cell-penetrating peptide (positive control, GRKKRRQRRRPPQ), whereas the free pre-S1 (9-24) peptide showed no activity. Furthermore, the secondary structure of the pre-S1 (9-24) peptide was investigated by CD

spectral analyses. As shown in Fig. 4C, the shape of the spectra, with a minimum at 200 nm and a shoulder at 222 nm, was indicative of a peptide with a high percentage of

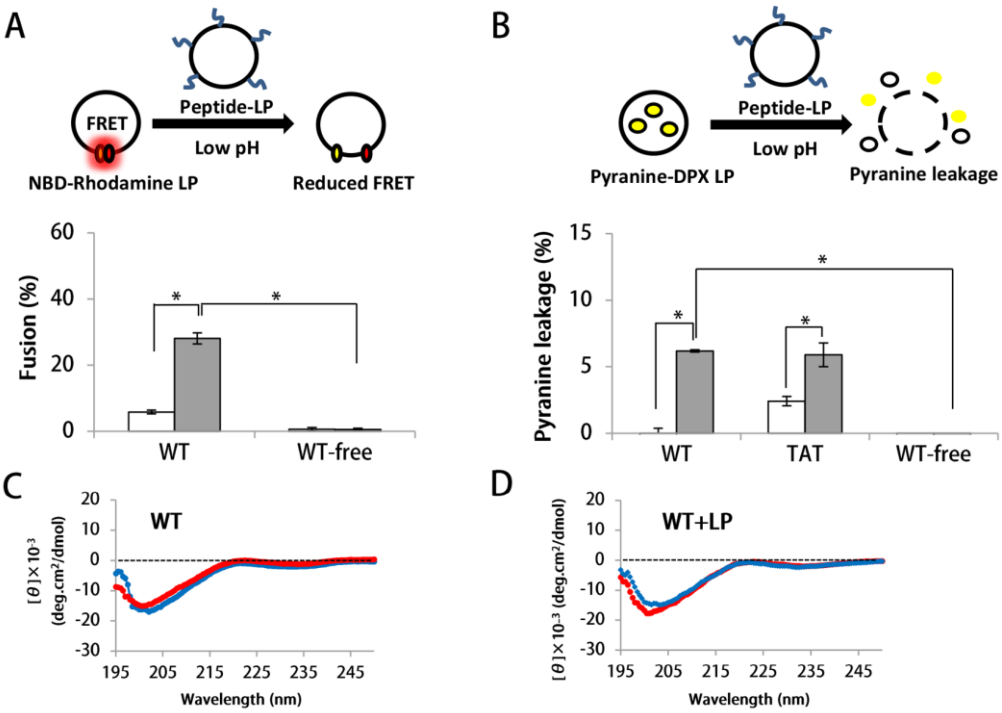

Fig. 4 Fusogenic and membrane disruption activity of the pre-S1 (9-24) peptide.

A. The fusogenic activity of the pre-S1 (9-24) peptide (wild type, WT) with or without displaying onto LPs, was measured by a lipid mixing assay at pH 7.4 (white bars) or pH 4.5 (gray bars). B. The membrane disruption activity of the pre-S1 (9-24) peptide and HIV Tat peptide (TAT) with or without displaying onto LPs was measured by a pyranine leakage assay at pH 7.4 (white bars) or pH 4.5 (gray bars). C and D. The CD spectra of the pre-S1 (9-24) peptide were obtained with (C) or without (D) LPs at pH 7.4 (blue line) and pH 5.3 (red line). Error bars represent SD. Student t-test; *, $p < 0.005$.

non-ordered structures (*i.e.*, random coil structure) under neutral and acidic conditions. In the presence of anionic LPs [DPPC:DPPE:DPPG-Na:cholesterol = 15:15:30:40 (mol)], no significant change was observed in the CD spectra of the peptide (Fig. 4D). Even in the presence of 40% (v/v) or 100% (v/v) TFE, which could mimic the environment in the lipid bilayer and induce α-helical formation, the CD spectra were not changed (data not shown). A high content of Pro residues (P10, P15, and P21) in the peptide might prevent the formation of rigid secondary structures. Collectively, these data indicated that the pre-S1 (9-24) peptide could exhibit a random coil structure and show both fusogenic and membrane disruption activity in a low pH-dependent manner exclusively on the membrane surface.

2.3.2. Mutational analysis of the pre-S1 (9-24) peptide

When endocytosed BNC and HBV move to late endosomes, they are considered to execute the endosomal escape of payloads and the uncoating process, respectively, through the interaction with the endosomal membrane. These processes are generally initiated by membrane fusion, followed by the disruption of the endosomal membrane and the BNC/HBV envelope membrane. Next, by using the LPs displaying pre-S1 (9-24) peptide mutants (Table 1), I performed a pyranine leakage assay using target LPs containing pyranine (fluorophore) and DPX (quencher) as a model of endosomes to investigate the essential aa required for the low pH-dependent membrane disruption activity. As shown in Fig. 5A, the membrane disruption activity of each peptide correlated well with the hydrophobicity of each peptide, calculated with the average ΔG value (bilayer to water, kcal/mol/residue) of each amino acid [14]. Based on the hydrophobic profile of the pre-S1 (9-24) peptide (Fig. 5B), the peptide (WT) was found to possess one

Table 1 The pre-S1 (9-24) mutated peptides and hydrophobicity.

Peptides (9-24)	Sequence	ΔG(kcal/mol/residue)
	Φ ΦΦ-+ Φ-* Φ	
WT	NPLGFFPDHQLDPAFG	-0.091
A11-15	AAAAA	-0.291
F13/14A	AA	-0.253
H17A	A	-0.041
P15/21A	A A	-0.056
P15A	A	-0.073
P21A	A	-0.073
D16/20L	L L	0.133
D16L	L	0.021
D20L	L	0.021
D16N	N	-0.040
D20N	N	-0.040
Δ9-12/21-24	---- ----	-0.204
Δ9-12	----	-0.094
Δ21-24	----	-0.163

[a]The hydrophobicity of each peptide was calculated using the Wimley-White hydrophobicity scale [14].

large hydrophobic cluster (I, from L11 to F14), one large hydrophilic cluster (from P15 to P21), and one small hydrophobic cluster (II, from A22 to G24) (Fig. 5B). The mutant

peptide lacking each hydrophobic cluster (Δ9-12, Δ21-24) showed decreased activity, and the mutant peptide lacking both hydrophobic clusters (Δ9-12/21-24) lost the activity completely (Fig. 5C). Furthermore, the mutant peptides harboring the Ala substitutions in the hydrophobic cluster I (F13/14A, 11-15A), resulting in decreased hydrophobicity, also lost the activity completely. These data strongly suggested that the hydrophobicity of the pre-S1 (9-24) peptide, especially hydrophobic cluster I, is tightly linked to the membrane disruption activity of the peptide.

2.3.3. Low pH-dependency of the pre-S1 (9-24) peptide

The pre-S1 (9-24) peptide showed low pH-dependent membrane disruption activity (*see* Fig. 4B). Therefore, I investigated which aa are responsible for sensing the acidity by using the LPs displaying pre-S1 (9-24) peptide mutants. Since some viral fusion proteins showed low pH-dependent conformational changes triggered by the protonation of acidic aa [15], either the D16 or D20 residue was substituted with an L residue, and subjected to the pyranine leakage assay (Fig. 6A). Both the D16L and D20L mutants showed higher membrane disruption activity than the WT peptide at pH 4.5, and retained low pH-dependency. The peptide harboring both the D16L and D20L mutations (D16/20L) showed comparable activity to the D16L and D20L mutants at pH 4.5 and, surprisingly, lost the low pH-dependency completely, indicating that both D16 and D20 function as low pH-sensing molecules. Furthermore, the mutations at residues D16/20L might generate an additional hydrophobic cluster between cluster I and II (Fig. 6B), while

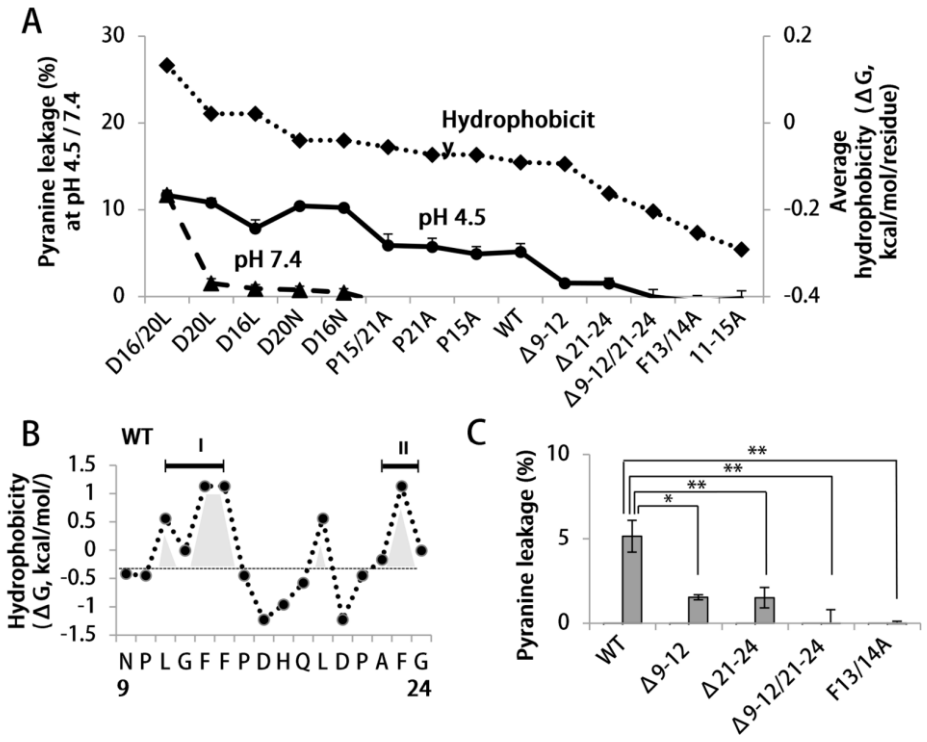

Fig. 5 Effect of hydrophobicity on the membrane disruption activity of the pre-S1 (9-24) peptide.

A. Relationship between the average hydrophobicity (diamond dotted line) and the membrane disruption activity at pH 7.4 (triangle dashed line) and pH 4.5 (circle line) of the mutated pre-S1 (9-24) peptides.The hydrophobicity was calculated using the Wimley-White hydrophobicity scale [14]. B. Hydrophobicity profile of the pre-S1 (9-24) peptide (wild type, WT). Hydrophobic clusters are indicated as I and II. C. Membrane disruption activity of mutant peptides (Δ9-12, Δ21-24, Δ9-12/21-24, and F13/14A). Error bars represent SD. Student t-test; **, $p < 0.005$, *, $p < 0.05$.

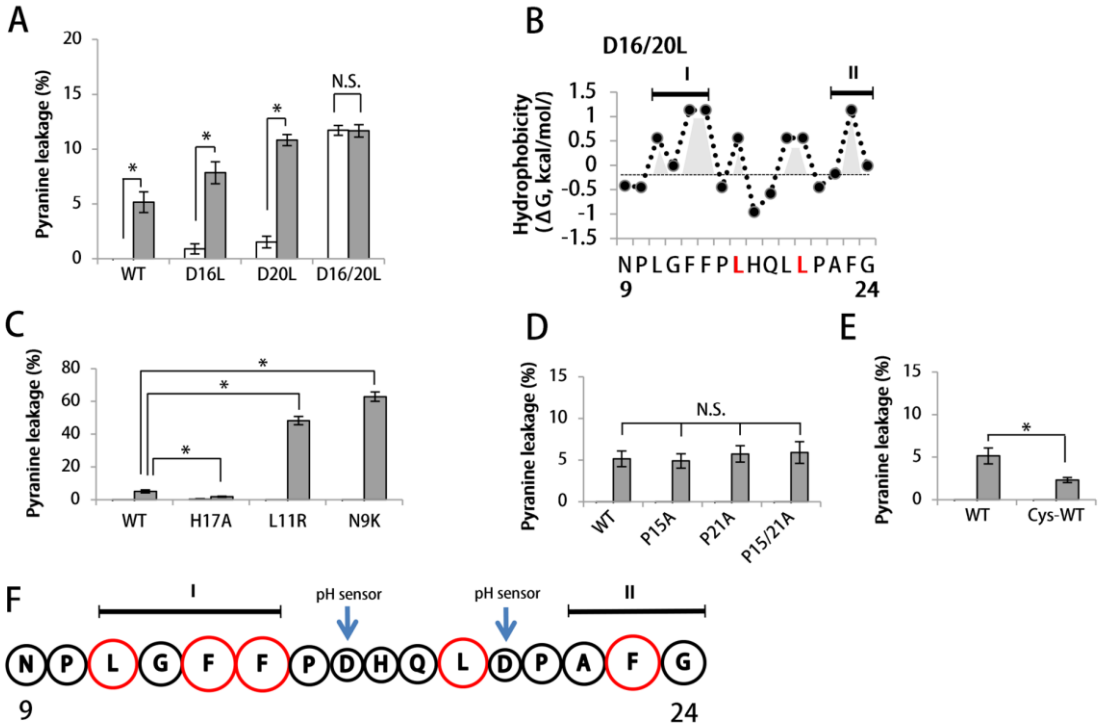

Fig. 6 Membrane disruption activity of mutated pre-S1 (9-24) peptides.

A. The membrane disruption activity of the wild type (WT), and the D16L, D20L, and D16/20L mutant peptides at pH 7.4 (white bars) and pH 4.5 (gray bars). B. Hydrophobicity profile of the D16/20L peptide. Hydrophobic clusters are indicated as I and II. C. The membrane disruption activity of the WT, and H17A, L11R, and N9K mutant peptides at pH 7.4 (white bars) and pH 4.5 (gray bars). D. The membrane disruption activity of the WT, and P15A, P21A, and P15/21A mutant peptides at pH 7.4 (white bars) and pH 4.5 (gray bars). E. The membrane disruption activity of the WT and Cys-WT mutant peptide at pH 7.4 (white bars) and pH 4.5 (gray bars). F. Schematic view of the pre-S1 (9-24) peptide. The diameter of each circle is based on the hydrophobicity of each amino acid [14]. Hydrophobic amino acids are indicated in red. Two D residues for sensing low pH are indicated with blue arrows. Numbers below amino acid sequences are the aa number of the L protein. Two hydrophobic clusters are indicated as I and II. Error bars represent SD. Student t-test; *, $p < 0.005$.

the D16/20L peptide exhibited a random coil structure at both pH 5.3 and pH 7.4 in the CD spectra (data not shown). These data corroborated that the hydrophobicity of the pre-S1 (9-24) peptide is critical for the membrane disruption activity.

2.3.4. His residue of the pre-S1 (9-24) peptide

When H17, a sole basic aa of the pre-S1 (9-24) peptide, was substituted with Ala, the membrane disruption activity at pH 4.5 was reduced to about one-third (Fig. 6C). Furthermore, the mutant peptides L11R and N9K, harboring additional basic aa, showed a significant increase in membrane disruption activity (about 9- and 12-fold). Since the surface of target LPs containing DPPG-Na (acidic phospholipid) is negatively charged (zata potential, -52 mV), these basic aa residues would likely be recruited to the proximal surface of the target LPs by electrostatic interaction, thereby enhancing their membrane disruption activity.

2.3.5. Pro residues of the pre-S1 (9-24) peptide

Pro residues are known to play an essential role in the fusogenic activity of some viral fusion proteins (*e.g.*, a Pro residue in the internal region of avian sarcoma/leukosis virus envelope protein [16], a Pro-rich motif in p15 fusion-associated small transmembrane protein of Orthoreovirus [17]). To examine if Pro residues (P15 and P21) of the pre-S1 (9-24) peptide are indispensable for the membrane disruption activity, each mutant peptide (P15A, P21A, and P15/21A) was displayed onto the LPs, and subjected to the pyranine leakage assay (Fig. 6D). However, these mutant peptides showed nearly equal levels of membrane disruption activity as observed for the WT peptide, indicating

that at least two of the Pro residues (P15 and P21) are not related to the low pH-dependent membrane disruption activity of the pre-S1 (9-24) peptide.

2.3.6. Membrane topology of the pre-S1 (9-24) peptide

The pre-S1 (9-24) peptide harbors a large hydrophobic cluster (cluster I) at the N-terminal half (*see* Fig. 5B) and the C-terminal C residue (artificial) for anchoring onto the surface of LPs, suggesting the involvement of cluster I in the initial interaction with target LPs. I therefore examined if the membrane topology of the peptide affects the membrane disruption activity by using the N-terminally C-fused pre-S1 (9-24) peptide (Cys-WT). As shown in Fig. 6E, the activity was reduced to about half, indicating that the membrane topology of the fused peptide is important for its membrane disruption activity, and that the N-terminal cluster I may predominantly interact with the membrane of target LPs.

2.4. Discussion

Using a pyranine leakage assay with LPs displaying mutant peptides, the pre-S1 (9-24) peptide was shown to possess low pH-dependent membrane disruption activity, while the peptide harbors a random coil structure regardless of the pH condition. The hydrophobicity of the whole structure was well correlated with its activity. Furthermore, most enveloped viruses possess fusion peptides, and the fusogenic activity is correlated well with their hydrophobicity [18]. For example, the influenza virus HA2 protein generated by proteolytic cleavage possesses an N-terminal hydrophobic α-helical cluster that is essential for membrane insertion [19]. The Newcastle disease virus F protein [20] and the simian immunodeficiency virus gp32 protein [21] were shown to have decreased fusogenic activity due to an aa mutation that lowered the hydrophobicity. These results

strongly suggested that the membrane insertion of the pre-S1 (9-24) peptide, an initial step of membrane fusion [1], is mainly driven by the hydrophobic interaction between the lipid bilayer and the peptide. With respect to the membrane topology of the peptide, the N-terminally anchored form of the pre-S1 (9-24) peptide showed lower membrane disruption activity (about half activity of the C-terminally anchored form; *see* Fig. 6E), implying that the N-terminal hydrophobic cluster I could insert into the target membrane predominantly.

Many fusion peptides of enveloped viruses exhibit an α-helical structure and, to a lesser extent, a β-sheet structure for interacting with the membrane [3,22], whereas the pre-S1 (9-24) peptide exhibited a random coil structure, which has been rarely found in the fusion peptides of flavivirus envelope protein [23]. The fusion peptide consisting of N-terminal and C-terminal hydrophobic clusters exhibits a random coil structure, even in the presence of the membrane. The aromatic-aromatic interaction between two aromatic aa residing in each cluster may be indispensable for the fusogenic activity [23]. In the pre-S1 (9-24) peptide, three aromatic aa found in hydrophobic clusters (F13 and F14 in cluster I, F23 in cluster II; Fig. 6F) may similarly contribute to the membrane disruption activity by stabilizing the whole peptide structure, which was in accordance with the results of the mutational study (Fig. 5C).

The low pH-dependent fusion peptides usually harbor each of three aa (D, E, and H) for sensing an acidic environment, leading to “Histidine-Cation” and “Anion-Anion” interactions [15]. These interactions affect the secondary structure of the fusion peptide and thereby enhance the fusogenic activity under low-pH condition. For example, the fusion peptide of influenza virus HA protein (GLFGAIAGFIENGWEGMIDG) showed a slight structure change by the protonation of E15 and D19 under low-pH conditions,

and then induced a fusogenic event in endosomes [3]. However, in the pre-S1 (9-24) peptide, both D16 and D20 were found to be independently responsible for low-pH sensing, whereas these residues did not significantly contribute to the structural change under the low-pH condition (Fig. 6A). These data strongly suggested that both D16 and D20 exclusively contribute to the enhancement of hydrophobicity of the pre-S1 (9-24) peptide by bridging between hydrophobic clusters I and II.

Recently, the pre-S protein (containing the whole pre-S1+pre-S2 region, without displaying onto LPs) was suggested to harbor low pH-dependent membrane destabilizing activity (*i.e.*, aggregation, membrane fusion, and membrane disruption). The protein exhibited a random coil structure even in the presence of the membrane and under the low-pH condition [24]. However, analysis using deletion mutants demonstrated that there is no specific region responsible for the membrane fusion in the pre-S1 region [9]. The discrepancy of the location of the fusion peptide in the pre-S1 region might be caused by the difference in the form of candidate proteins and peptides (free form *versus* LP-anchored form). Because the membrane fusion occurs between two membranes by the interaction of a membrane-anchored fusion peptide (like viral envelope proteins), it is considered that the LP-anchored form of a fusion peptide can more precisely replicate the viral envelope protein.

References

1. S.C. Harrison, Viral membrane fusion, *Virology*, 2015, 479-480, 498-507.
2. D.S. Dimitrov, Virus entry: molecular mechanisms and biomedical applications, *Nature Reviews Microbiology*, 2004, 2, 109-122.

3. X. Han, J.H. Bushweller, D.S. Cafiso, L.K. Tamm, Membrane structure and fusion-triggering conformational change of the fusion domain from influenza hemagglutinin, *Nature Structural & Molecular Biology*, 2001, 8, 715-720.

4. P. Tiollais, C. Pourcel, A. Dejean, The hepatitis B virus, *Nature*, 1985, 317, 489-495.

5. S. Urban, R. Bartenschlager, R. Kubitz, F. Zoulim, Strategies to inhibit entry of HBV and HDV into hepatocytes, *Gastroenterology*, 2014, 147, 48-64.

6. S. Oess, E. Hildt, Novel cell permeable motif derived from the PreS2-domain of hepatitis-B virus surface antigens, *Gene Therapy*, 2000, 7, 750–758.

7. I. Rodriguez-Crespo, J. Gomez-Gutierrez, M. Nieto, D.L. Peterson, F. Gavilanes, Prediction of a putative fusion peptide in the S protein of hepatitis B virus, *Journal of General Virology*, 1994, 75, 637-639.

8. I. Rodríguez-Crespo, E.Núñez, J.Gómez-Gutierrez, B.Yélamos, J.P. Albar,D.L. Peterson, F. Gavilanes, Phospholipid interactions of a putative fusion peptide of hepatitis B virus surface antigen S protein, *Journal of General Virology*, 1995, 76, 301–308.

9. C.L. Delgado, E. Nunez, B. Yelamos, J. Gomez-Gutierrez, D.L. Peterson, F. Gavilanes, Study of the putative fusion regions of the preS domain of hepatitis B virus, *Biochimica et Biophysica Acta*, 2015, 1848, 895-906.

10. T. Yamada, Y. Iwasaki, H. Tada, H. Iwabuki, M.K. Chuah, T. VandenDriessche, H. Fukuda, A. Kondo, M. Ueda, M. Seno, K. Tanizawa, S. Kuroda, Nanoparticles for the delivery of genes and drugs to human hepatocytes, *Nature Biotechnology*, 2003, 21, 885-890.

11. M. Yamada, A. Oeda, J. Jung, M. Iijima, N. Yoshimoto, T. Niimi, S.Y. Jeong, E.K. Choi, K. Tanizawa, S. Kuroda, Hepatitis B virus envelope L protein-derived bio-

nanocapsules: mechanisms of cellular attachment and entry into human hepatic cells, *Journal of Controlled Release*, 2012, 160, 322-329.

12. M. Somiya, S. Kuroda, Development of a virus-mimicking nanocarrier for drug delivery systems: The bio-nanocapsule, *Advanced Drug Delivery Reviews*, 2015, 95, 77-89.
13. M. Somiya, Y. Sasaki, T. Matsuzaki, Q. Liu, M. Iijima, N. Yoshimoto, T. Niimi, A.D. Maturana, S. Kuroda, Intracellular trafficking of bio-nanocapsule-liposome complex: Identification of fusogenic activity in the pre-S1 region of hepatitis B virus surface antigen L protein, *Journal of Controlled Release*, 2015, 212, 10-18.
14. W.C. Wimley, S.H. White, Experimentally determined hydrophobicity scale for proteins at membrane interfaces, *Nature Structural & Molecular Biology*, 1996, 3, 842-848.
15. J.S. Harrison, C.D. Higgins, M.J. O'Meara, J.F. Koellhoffer, B.A. Kuhlman, J.R. Lai, Role of electrostatic repulsion in controlling pH-dependent conformational changes of viral fusion proteins, *Structure*, 2013, 21, 1085-1096.
16. S.E. Delos, J.M. Gilbert, J.M. White, The central proline of an internal viral fusion peptide serves two important roles, *Journal of Virology*, 2000, 74, 1686-1693.
17. D. Top, J.A. Read, S.J. Dawe, R.T. Syvitski, R. Duncan, Cell-cell membrane fusion induced by p15 fusion-associated small transmembrane (FAST) protein requires a novel fusion peptide motif containing a myristoylated polyproline type II helix, *Journal of Biological Chemistry*, 2012, 287, 3403-3414.
18. E.I. Pecheur, J. Sainte-Marie, A. Bienvenüe, D. Hoekstra, Peptides and membrane fusion: towards an understanding of the molecular mechanism of protein-induced fusion, *Journal of Membrane Biology*, 1999, 167, 1-17.

19. C. Harter, P. James, T. Bachi, G. Semenza, J. Brunner, Hydrophobic binding of the ectodomain of influenza hemagglutinin to membranes occurs through the "fusion peptide", *Journal of Biological Chemistry*, 1989, 264, 6459-6464.
20. T. Sergel-Germano, C. McQuain, T. Morrison, Mutations in the fusion peptide and heptad repeat regions of the Newcastle disease virus fusion protein block fusion, *Journal of Virology*, 1994, 68, 654-7658.
21. M.L. Bosch, P.L. Earl, K. Fargnoli, S. Picciafuoco, F. Giombini, F. Wong-Staal, G. Franchini, Identification of the fusion peptide of primate immunodeficiency viruses, *Science*, 1989, 244, 694-697.
22. A.L. Lai, A.E. Moorthy, Y. Li, L.K. Tamm, Fusion activity of HIV gp41 fusion domain is related to its secondary structure and depth of membrane insertion in a cholesterol-dependent fashion, *Journal of Molecular Biology*, 2012, 418, 3-15.
23. Y.S. Mendes, N.S. Alves, T.L. Souza, I.P. Sousa, Jr., M.L. Bianconi, R.C. Bernardi, P.G. Pascutti, J.L. Silva, A.M. Gomes, A.C. Oliveira, The structural dynamics of the flavivirus fusion peptide-membrane interaction, *PLoS One*, 2012, 7, e47596.
24. E. Nunez, B. Yelamos, C. Delgado, J. Gomez-Gutierrez, D.L. Peterson, F. Gavilanes, Interaction of preS domains of hepatitis B virus with phospholipid vesicles, *Biochimica et Biophysica Acta*, 2009, 1788, 417-424.

Chapter III

A Hepatitis B Virus-derived Human Hepatic Cell-specific Heparin-binding Peptide: Identification and Application to a Drug Delivery System

3.1. Introduction

Drug delivery system (DDS) nanocarriers that are systemically administered should escape from the mononuclear phagocyte system (MPS), which includes monocytes, macrophages, and Kupffer cells [1, 2], and then deliver their payloads to target tissues specifically [3]. Furthermore, they should trigger endocytosis and then release their payloads into the cytoplasm by perturbing the endosomal membrane [4, 5]. Thus far, conventional synthetic nanocarriers have not fully demonstrated these functions that are found in the early infection machineries of naturally occurring viruses. In the last decade, viruses have been engineered as DDS nanocarriers for the delivery of drugs and/or genes. Innate properties of viruses, such as broad tissue tropism, diverse cellular receptors, high immunogenicity, carcinogenicity, and limited payload capacity, have hampered their clinical application [6]. Furthermore, it is sometimes difficult to obtain large amount of these viruses in mass-scale production. These situations have led us to reconsider using intact viruses and to instead develop synthetic nanoparticles equipped with viral early infection machinery with stringent specificity for target cells and tissues.

Hepatitis B virus (HBV) is a ~42-nm enveloped DNA virus that can specifically infect human hepatic cells. There are three types of envelope proteins on the surface of HBV: small (S), middle (M, pre-S2 + S region), and large (L, pre-S1 + pre-S2 + S region) proteins [7]. HBV is believed to interact first with heparan sulfate proteoglycan (HSPG)

on human hepatocytes [8, 9], promptly move to interacting with sodium taurocholate-cotransporting polypeptide (NTCP; an essential receptor for HBV infection) [10], and then enter these cells by receptor-mediated endocytosis [11]. Our group have established an HBV-mimicking nanoparticle, bio-nanocapsule (BNC), which is composed of HBV envelope L proteins embedded in a lipid bilayer and demonstrates human liver targeting, cell entry, and endosomal escape [12, 13]. BNCs can deliver drugs and genes to human hepatic tissues specifically and efficiently *in vitro* and *in vivo* [14]. Furthermore, BNCs can fuse with liposomes (LPs) and form BNC-virosomes under acidic conditions to deliver doxorubicin (DOX) to human hepatic tumors in xenograft mice and efficiently inhibit tumor growth [15-17]. Although BNCs and BNC-virosomes are promising HBV-mimicking nanoparticles, biologics-related issues, such as immunogenicity, quality control, and production costs, have obstructed the conduct of clinical research on these drugs. Thus, as next-generation HBV-mimicking nanoparticles, conventional synthetic nanocarriers should deploy the early infection machinery of HBV by displaying functional domains, such as cell targeting peptide, cell entry peptide, and an endosomal escaping peptide.

To date, several functional domains responsible for early infection have been identified in the HBV L protein. First, polymerized-albumin receptor (PAR) in the pre-S2 region [18] has been shown to contribute to the escape from MPS by recruiting polymerized human serum albumin [13]. Second, the human hepatic cell recognition site at the N-terminal peptide of the pre-S1 region (from Pro-10 to Pro-36) [19] and NTCP-binding site at the myristoylated N-terminal peptide of the pre-S1 region (from Gly-2 to Val-47; myr-pre-S1(2–47)) [10] both contribute to cellular targeting and entry. Third, the low pH-dependent fusogenic domain of the N-terminal peptide in the pre-S1 region (from

Asn-9 to Ala-24) contributes to endosomal escape [20,21]. Recently, LPs modified with the NTCP-targeting peptide have been used as a human hepatic tissue-specific nanocarrier [22]; however, our group found that HSPG, rather than cell-surface NTCP, is responsible for the initial attachment of HBV to cells and induction of endocytosis [23]. HBV cell entry can be blocked by heparin completely, indicating that the interaction of HBV with human hepatic tissues is mediated by heparin [8]. Recently, several groups have reported that the pre-S region contains a heparin-binding domain indispensable for initial cellular attachment of HBV [24, 25]. Thus, even if conventional synthetic nanocarriers harbor the HBV-derived functional domains mentioned above, it is still necessary to introduce the heparin-dependent cellular attachment domain to maximize the efficiency of initial attachment. In this study, I identified a novel heparin-binding site in the pre-S1 region using peptide-displaying LPs. The heparin-binding peptide (from Pro-30 to Pro-42) showed higher specificity to human hepatic cells than other heparin-binding peptides and induced endocytosis efficiently. Furthermore, I showed that the peptide-displaying LPs are promising HBV-mimicking nanoparticles for human hepatic cell-specific drug delivery.

3.2. Experimental Procedures

3.2.1. Peptides

The HBV pre-S1-derived peptide (encompassing myristoylated Gly-2 to Val-77, with C-terminal Cys), its truncated mutant peptides (with C-terminal Cys), and conventional heparin-binding peptides (human immunodeficiency virus (HIV, gp120, RPNNNTRKRIRC), vitronectin (GKKQRFRHRNRKGC)) were synthesized by Synpeptide Co. Ltd. (Shanghai, China) and SCRUM Inc. (Tokyo, Japan).

3.2.2. Preparation of peptide-displaying liposomes

To prepare maleimide-displaying LPs, ethanol containing dipalmitoylphosphatidylcholine (DPPC; NOF, Tokyo, Japan), cholesterol (Nacalai Tesque, Kyoto, Japan), and N-(3-maleimide-1-oxopropyl)-L-α-phosphatidylethanolamine (DOPE-MAL; NOF) were injected at a molar ratio of 55:40:5 into 10 mM Tris-HCl buffer (pH 8.0) with gentle stirring at room temperature and then subjected to a Sephadex G-25 gel filtration column (GE Healthcare, Buckinghamshire, UK) equilibrated with phosphate-buffered saline (PBS). To prepare PEGylated maleimide-displaying LPs, a mixture of DPPC, cholesterol, and N-[(3-maleimide-1-oxopropyl) aminopropyl polyethyleneglycol-carbamyl] distearoylphosphatidyl-ethanolamine (DSPE-PEG-MAL) at a molar ratio of 55:40:5 were processed by microfluidics technique using a NanoAssemblr Benchtop system (Precision Nanosystems, Vancouver, Canada). Peptides with C-terminal Cys were displayed on the LP surface using a maleimide-thiol coupling reaction [21]. Peptide-displaying LPs were labeled with the lipophilic dye CellVue Claret (Sigma-Aldrich, St Louis, MO, USA).

3.2.3. Physicochemical analyses

The size, polydispersity index (PDI), and ς-potential of LPs were measured with a Zetasizer Nano ZS (Malvern, Worcestershire, UK). The concentration of lipids in LPs was calculated with the cholesterol content determined using a Cholesterol E-Test Wako kit (Wako, Osaka, Japan).

3.2.4. Cell culture

Human hepatocellular carcinoma-derived HepG2 cells expressing NTCP

(HepG2/NTCP) were kindly provided by Dr. Ryosuke Suzuki (National Institute of Infectious Diseases, Tokyo, Japan). Human hepatocellular carcinoma-derived NuE cells were a gift from Prof. Takushi Tadakuma (National Defense Medical College, Tokorozawa, Japan). Primary human hepatocytes (PHH, originating from a 54-year-old Caucasian female) were purchased from Lonza (Basel, Switzerland). Human embryonic kidney-derived HEK293T cells, rat hepatocellular carcinoma-derived MH1C1 cells, human colon carcinoma-derived WiDr cells, human lung carcinoma-derived A549 cells, and human cervical carcinoma-derived HeLa cells were purchased from RIKEN Cell Bank (Tsukuba, Japan). Cells were maintained in Ham's F-12/Dulbecco's modified Eagle's medium (DMEM) (50%/50%, v/v, Nacalai Tesque, Kyoto, Japan) supplemented with 10% (v/v) fetal bovine serum (FBS, Sigma-Aldrich) at 37 ℃ in a humidified atmosphere containing 5% (v/v) CO_2.

3.2.5. Flow cytometry analysis

Approximately 1.0×10^5 HepG2 cells were seeded in 6-well plates (Corning Inc., New York, NY, USA) and incubated in culture medium containing 3% (v/v) DMSO at 37 ℃ for at least 24 h. Cells were incubated with CellVue-labeled peptide-displaying LPs (10 μg/mL as lipid) at 37 ℃ for 6 h, washed twice with Dulbecco's PBS (D-PBS, Nacalai Tesque), and then analyzed using a FACS Canto II flow cytometer (BD Biosciences, San Diego, CA, USA). To evaluate the effect of heparin on cellular attachment of peptide-displaying LPs, heparin sodium salt (10 μg/mL final, Nacalai Tesque) was added to the culture medium 5 min before the addition of CellVue-labeled peptide-displaying LPs (10 μg/mL as lipid). To analyze the endocytosis pathway of peptide-displaying LPs, cells were treated with the endocytosis inhibitor chlorpromazine (12.5 μg/ml, 30 min) or

amiloride (1 mM, 15 min), and then incubated with CellVue-labeled peptide-displaying LPs (10 μg/mL as lipid) for 6 h.

3.2.6. Intracellular trafficking analysis

Approximately 5.0 × 10^4 HepG2 or HepG2/NTCP cells/well were seeded in 8-well glass bottomed chamber slides (Corning Inc.), and incubated in culture medium containing 3% DMSO for 24 h. After fixation and staining with Hoechst 33342 (Nacalai Tesque), cell-surface NTCP was visualized with a rabbit polyclonal anti-NTCP antibody (HPA042727, Sigma-Aldrich) and an Alexa Fluor-488 labeled goat anti-rabbit IgG (H+L) secondary antibody (Thermo Fisher Scientific, Waltham, MA, U.S.A).

Approximately 5.0 × 10^4 HepG2 or HepG2-NTCP cells/well grown on 8-well glass-bottomed chamber slides were incubated in culture medium containing 3% DMSO for 24 h, and then incubated in culture medium containing 5 μg/mL (as a lipid) of CellVue-labeled peptide-LPs at 37 ℃ for 5.5 h, followed by a 30-min incubation with 50 nM LysoTracker Red (Thermo Fisher Scientific, Waltham, MA, USA). After fixation with 4% (w/v) paraformaldehyde, cells were stained with Hoechst 33342 (Nacalai Tesque). The fluorescence images obtained by a confocal laser scanning microscope (LSM) FV-1000 (Olympus, Tokyo, Japan) were analyzed using ImageJ version 1.47g software (National Institutes of Health, Bethesda, MA, USA).

For visualizing intracellular localization of DOX, approximately 5.0 × 10^4 HepG2 cells/well grown on 8-well glass-bottomed chamber slides at 37 ℃ for 24h, then incubated with DOX, LPs containing DOX, pre-S1(30–42)-displaying LPs containing DOX, myr-pre-S1(2–47)-displaying LPs containing DOX, and pre-S1(47–77)-displaying LPs containing DOX (25 μg/mL as DOX) for 8 h. The fluorescence derived from DOX

and Hoechst 33342 was observed under confocal LSM FV-1000D.

To label early endosomes and late endosomes/lysosomes, HepG2 cells were fixed with 4% (w/v) paraformaldehyde, stained with Hoechst 33342, permeabilized with 0.1% (w/v) Triton X-100 (Wako), and then treated with a mouse monoclonal anti-EEA1 (early endosome antigen-1) antibody (Abcam, Cambridge, UK) or mouse monoclonal anti-LAMP2 (lysosome-associated membrane protein-2) antibody (Abcam). Both EEA1 and LAMP2 were visualized with an Alexa Fluor 555-labeled goat anti-mouse IgG secondary antibody (Sigma-Aldrich).

3.2.7. Evaluation of cell-surface proteoglycans

Approximately 5.0×10^4 HepG2 cells/well were grown on 8-well glass bottomed chamber slides for 24 h. To evaluate the effect of heparin on cellular attachment of peptide-displaying LPs, cells pre-treated with heparin sodium salt (10 μg/mL; see above) were incubated with CellVue-labeled peptide-LPs at 37 ℃ for 6 h, observed under LSM, and then analyzed using ImageJ software. For the removal of sulfate groups on cell-surface HSPG, cells were incubated with sodium chlorate (100 mM, Nacalai Tesque) for 16 h and with CellVue-labeled peptide-LPs at 37 ℃ for the next 6 h, and then observed under LSM. For the ablation of heparin sulfate groups on cell-surface HSPG, cells were incubated with 8 units/mL heparinase I (Sigma-Aldrich) for 60 min at 37 ℃ without serum, incubated with CellVue-labeled peptide-LPs at 37 ℃ for 6 h, and then subjected to LSM observation.

3.2.8. Heparin-binding assay

Peptide-displaying LPs (20 μg/mL, as a lipid) labeled with 1,1'-dioctadecyl-

3,3,3',3'-tetramethylindodicarbocyanine, 4-chlorobenzenesulfonate salt (DiD; Thermo Fisher Scientific) were incubated with 50 μL (50% slurry) of Heparin Sepharose 6 beads (GE Healthcare) or Sepharose 6B beads (GE Healthcare) in PBS for 1 h, and then washed twice with PBS. The fluorophores were eluted from bound LPs with PBS containing 0.1% (v/v) Triton X-100, and their fluorescence intensity was measured using a Varioskan fluorescence microplate reader (Thermo Electron, Vantaa, Finland).

3.2.9. Encapsulation of doxorubicin into LPs

Doxorubicin (DOX; Sigma-Aldrich) was encapsulated into LPs using a remote loading method [17, 26]. Free DOX was removed by a Sephadex G-25 gel filtration column equilibrated with 10 mM HEPES buffer (pH 7.4) containing 100 mM NaCl and 3.4% (w/v) sucrose. Following disruption with 0.1% (w/v) sodium dodecyl sulfate (SDS) and 0.1 N HCl, the total DOX concentration was calculated from the fluorescence intensity derived from DOX (excitation at 475 nm; emission at 515 nm), which was measured using a Varioskan fluorescence microplate reader.

3.2.10. Cytotoxicity assay

HepG2 cells (approximately 5×10^3 cells/well) seeded in 96-well cell culture plates (Nalge Nunc, Naperville, IL) were cultured for 24 h, and then treated with DOX, DOX-containing LPs, and DOX-containing peptide-displaying LPs at DOX concentrations of 0.195–25 μg/mL at 37°C for 8 h. As a control, cells were treated with 40 μg/mL of LPs without DOX encapsulation. Following a fresh medium exchange, cells were further incubated at 37 ℃ for 24 h. Cell viability was determined using WST-8 assay reagent (Nacalai Tesque) according to the manufacturer's protocol. The formation of

tetrazolium salts from WST-8 was measured using a Varioskan fluorescence microplate reader.

3.3. Results

3.3.1. Identification of the cellular attachment domain in the pre-S1 region

Because the pre-S region is responsible for the heparin-dependent binding of HBV [24, 25], I delineated the HepG2 cell-attachment domain using truncated pre-S1

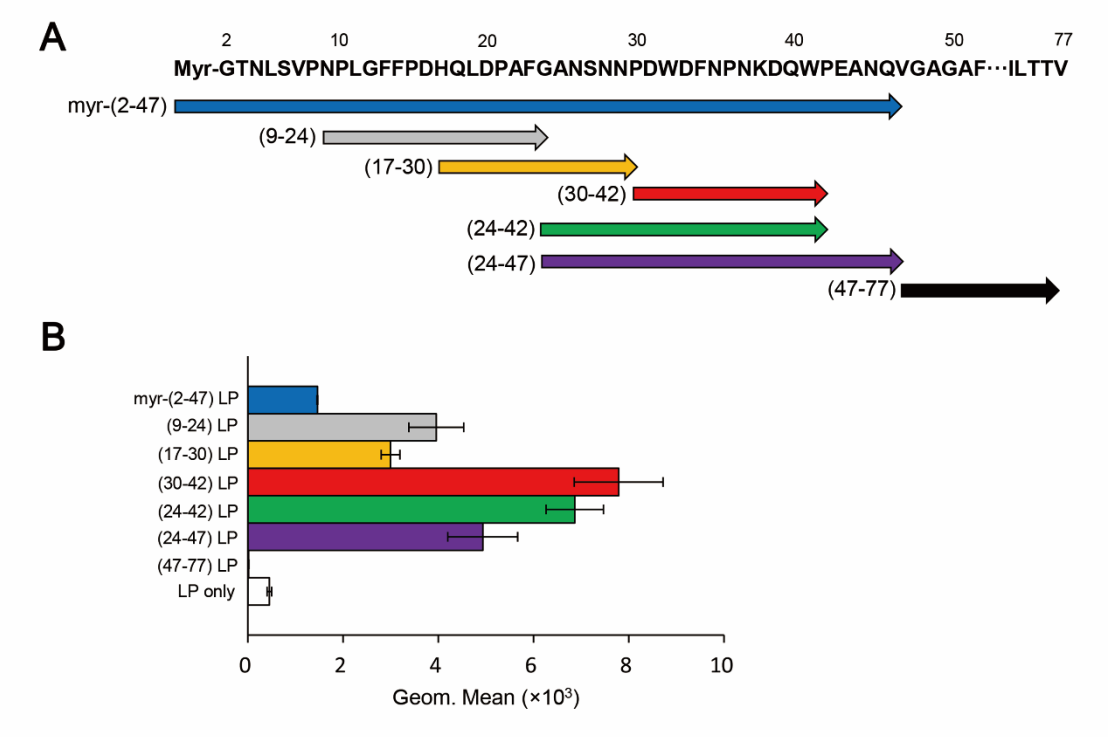

Fig. 7 Delineation of the cellular attachment domain in the pre-S1 region.
Pre-S1-derived synthetic peptides (A) were displayed on LPs, and then subjected to a cellular attachment analysis (B) using HepG2 cells. Blue, myr-(2–47) peptide; gray, (9–24) peptide; yellow, (17–30) peptide; red, (30–42) peptide; green, (24–42) peptide; purple, (24–47) peptide; and black, (47–77) peptide. N=3, error bars represent SDs.

peptide-displaying CellVue-labeled LPs (Fig. 7A). The size, PDI, and ς-potential of each sample was shown in Fig. 8. All samples exhibited a comparable size (from ~100 nm to

~200 nm; PDI from ~0.2 to ~0.3) and negative charge (from ~ -30 mV to ~ -50 mV).

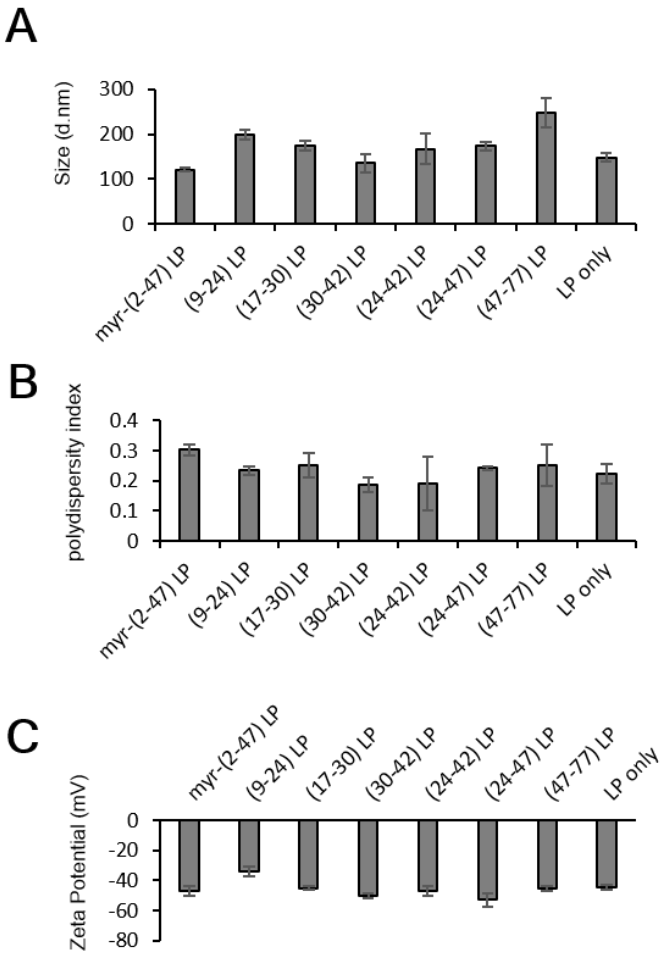

Fig. 8 Physicochemical analyses of peptide-displaying LPs.

LPs were modified with different pre-S1 peptide. Particle size, PDI, and ς-potential were measured by Zetasizer Nano ZS. N=3, error bars represent SDs.

After incubation at 37 ℃ for 6 h, cells were subjected to flow cytometry analysis. Compared with the myr-pre-S1(2–47) peptide, truncated peptides encompassing Asn-9 to Val-47 exhibited higher cellular attachment activity with HepG2 cells, whereas pre-S1(47–77) peptide exhibited no activity (Fig. 7B). The pre-S1(30-42) peptide showed the highest affinity for HepG2 cells.

3.3.2. Cellular attachment of pre-S1-derived peptide-displaying LPs

Pre-S1-derived peptide-displaying LPs were applied to HepG2 cells with or without NTCP overexpression (Fig. 9). After incubation at 37℃ for 6 h, cells were observed under LSM (Fig. 10A). Pre-S1(30-42)-displaying LPs exhibited significantly higher cellular attachment activity than myr-pre-S1(2-47)-displaying LPs, which was not affected by NTCP overexpression (Fig. 10B). Meanwhile, pre-S1(2–47)-displaying LPs showed a comparable level of cellular attachment activity to myr-pre-S1(2–47)-displaying LPs in HepG2 cells, but slightly lower activity in HepG2/NTCP cells (Fig. 10B). These results indicated that cell-surface NTCP does not substantially contribute to the cellular attachment of pre-S1(30-42)-displaying LPs. These data indicated that the pre-S1(30–42) domain plays a pivotal role in the initial cellular attachment of HBV in a NTCP-independent manner and that the flanking regions of the pre-S1(30–42) domain

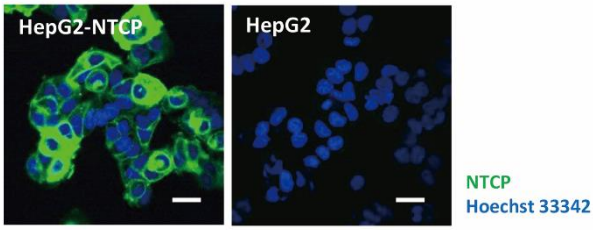

Fig. 9 Immunostaining of cell-surface NTCP.

Scale bars represent 20 μm.

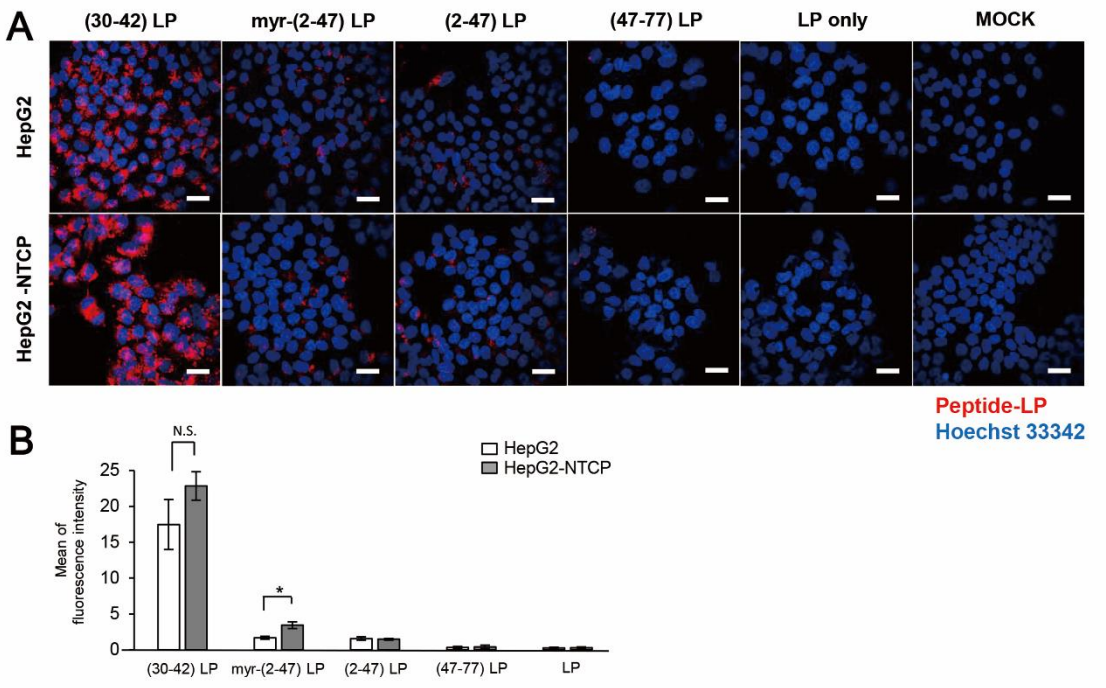

Fig. 10 Cellular attachment of pre-S1-derived peptide-displaying LPs.

Pre-S1-derived peptide-displaying CellVue-labeled LPs were incubated with HepG2 cells with or without NTCP expression. After staining nuclei with Hoechst 33342 (blue), CellVue-derived fluorescence (red) was observed under a confocal laser scanning microscope (A). Peptides used were the pre-S1(30–42) peptide, myr-pre-S1(2–47) peptide, pre-S1(2–47) peptide, and pre-S1(47–77) peptide. Scale bars represent 20 μm. The amounts of fluorophore in each cell were determined using the ImageJ program (B). N=3, error bars represent SDs. Student's t-test; *, $p < 0.005$. N.S., not significant.

may suppress cellular attachment activity.

3.3.3. Cell entry and intracellular trafficking of pre-S1(30–42)-displaying LPs

Conjugation of pre-S1(30-42) peptide on the LPs was optimized. The sizes, PDI and ς-potential of pre-S1(30-42)-displaying LPs with different ratio of DOPE-MAL were shown (Fig. 11). The results indicated that pre-S1(30-42)-displaying LPs with less than

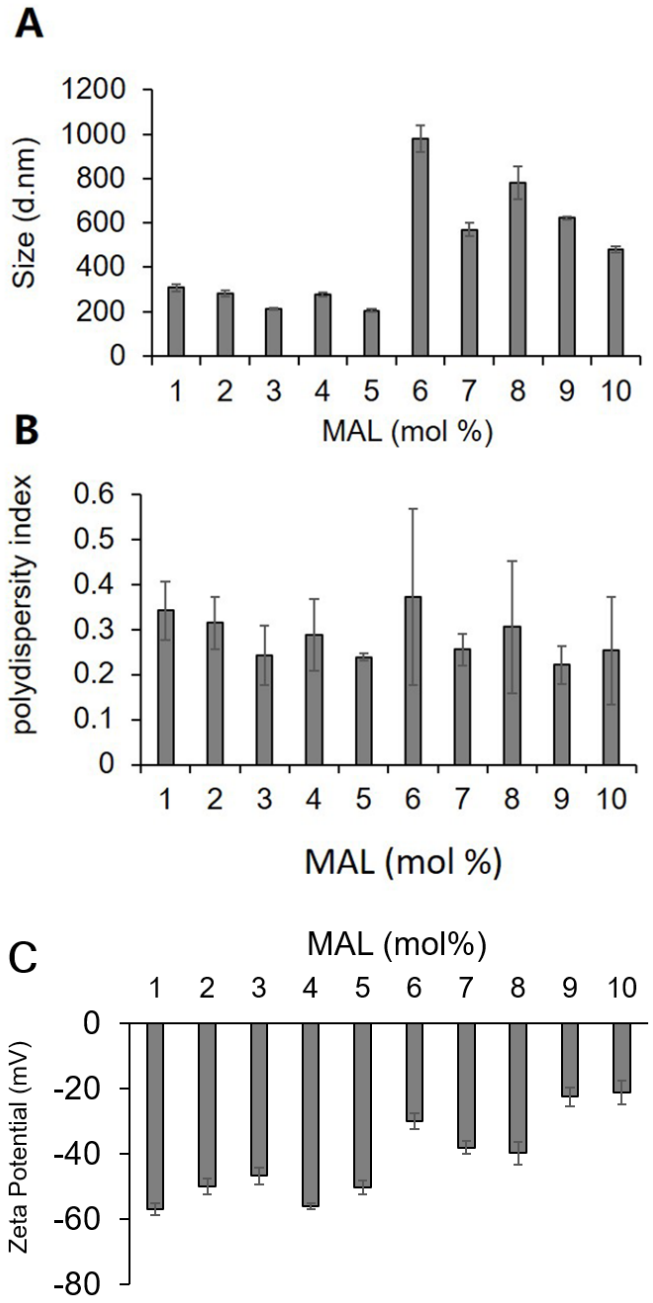

Fig. 11 Optimization of pre-S1(30-42)-displaying LPs.

Pre-S1(30-42) peptide was conjugated on the LPs containing different amount of DOPE-MAL. Particle size, PDI and ς-potential were measured by Zetasizer Nano ZS. N=3, error bars represent SDs.

5 mol% of DOPE-MAL exhibited optimal particle size and PDI. HepG2 cells were

incubated with CellVue-labeled pre-S1(30–42)-displaying LPs at 37℃ for 6 h, and then subjected to flow cytometry. The pre-S1(30-42)-displaying LPs with 5 mol% of DOPE-MAL exhibited higher cellular attachment activity with HepG2 cells than that of 1 to 4 mol% DOPE-MAL (Fig. 12). No significant difference was found in pre-S1(30-42)-

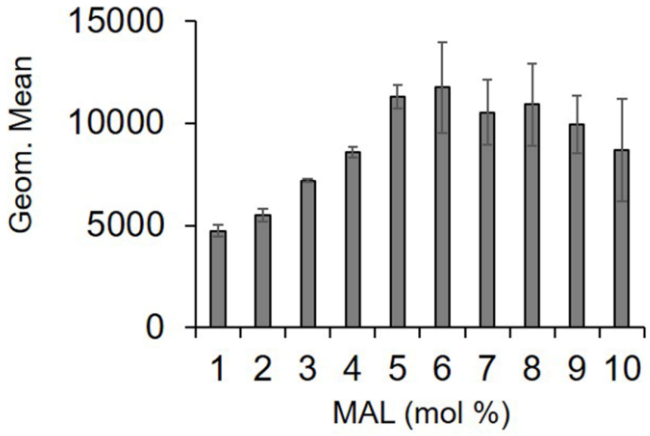

Fig. 12 Cellular attachment of pre-S1(30-42)-displaying LPs with different DOPE-MAL ratios in HepG2 cells.

N=3, error bars represent SDs.

displaying LPs with 5 to 10 mol% of DOPE-MAL, indicating that pre-S1(30-42)-displaying LPs with 5 mol% DOPE-MAL is optimal condition for cellular delivery. Consequently, pre-S1(30-42)-displaying LPs with 5 mol% of DOPE-MAL were used for further experiments.

HepG2 cells were incubated with CellVue-labeled pre-S1(30–42)-displaying LPs at 37℃ for 6 h, and then trypsinized at 37℃ for 20 min to remove extracellular proteins and LPs [23]. The cells were next subjected to flow cytometry assay. As shown in Fig. 13A, no significant difference was found between trypsinized and intact HepG2 cells, indicating that nearly all pre-S1(30–42)-displaying LPs were incorporated into HepG2 cells. When HepG2 cells were incubated with CellVue-labeled pre-S1(30–42)-

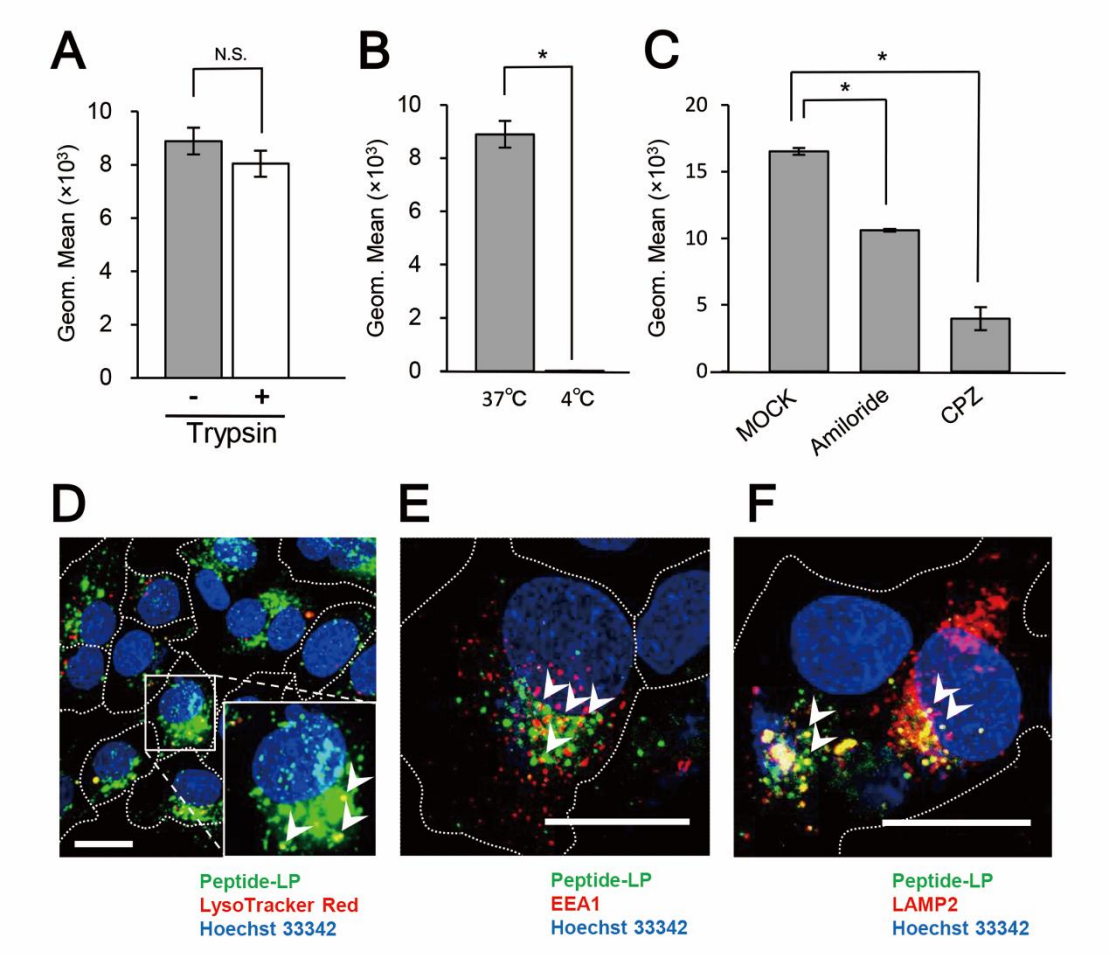

Fig. 13 Intracellular trafficking analysis of pre-S1 (30-42)-displaying LPs.

HepG2 cells were incubated with pre-S1 (30–42)-displaying CellVue-labeled LPs under various conditions (with trypsinization (A), incubation at 4℃ (B), and endocytosis inhibitors (C)), and then analyzed by flow cytometry. N=3, error bars represent SDs. Student's t-test; *, $p < 0.005$. Subcellular localizations of pre-S1 (30–42)-displaying CellVue-labeled LPs in HepG2 cells. Lysotracker (D), EEA1 (E), and LAMP2 (F) were analyzed under a confocal laser scanning microscope. Scale bars represent 20 μm.

displaying LPs at 4℃ for 1 h, weak fluorescence was observed in the cells (Fig. 13B), suggesting that the cell entry of pre-S1 (30–42)-displaying LPs is temperature dependent. Next, HepG2 cells were treated with endocytosis inhibitors (chlorpromazine or amiloride), and then with CellVue-labeled pre-S1(30–42)-displaying LPs at 37℃ for 6 h. As shown in Fig. 13C, both inhibitors (amiloride and chlorpromazine (CPZ)) significantly repressed

the incorporation of pre-S1(30–42)-displaying LPs, indicating that cell entry is mainly driven by clathrin-mediated endocytosis and micropinocytosis, similar to that of BNCs and HBV virions [27, 28].

The materials incorporated by receptor-mediated endocytosis are mainly sorted to late endosomes/lysosomes via early endosomes [29]. HepG2 cells were incubated with CellVue-labeled pre-S1(30–42)-displaying LPs at 37℃ for 6 h, and then subjected to LSM observation. The pre-S1(30–42)-displaying LPs were found to partially co-localize with LysoTracker Red (Fig. 13D), early endosome marker EEA-1 (Fig. 13E), and late endosome/lysosome marker LAMP-2 (Fig. 13F). Time course study of the uptake of pre-S1(30–42)-displaying LPs, pre-S1(47–77)-displaying LPs and unmodified LPs in the HepG2 cells were shown in Fig. 14. I found that the cellular attachment and entry of pre-S1(30–42)-displaying LPs was increased in a time-dependent manner. The intracellular trafficking of unmodified LPs was evaluated as a control (Fig. 15A). These data indicated that pre-S1(30–42)-displaying LPs could enter HepG2 cells with the help of endocytosis machinery.

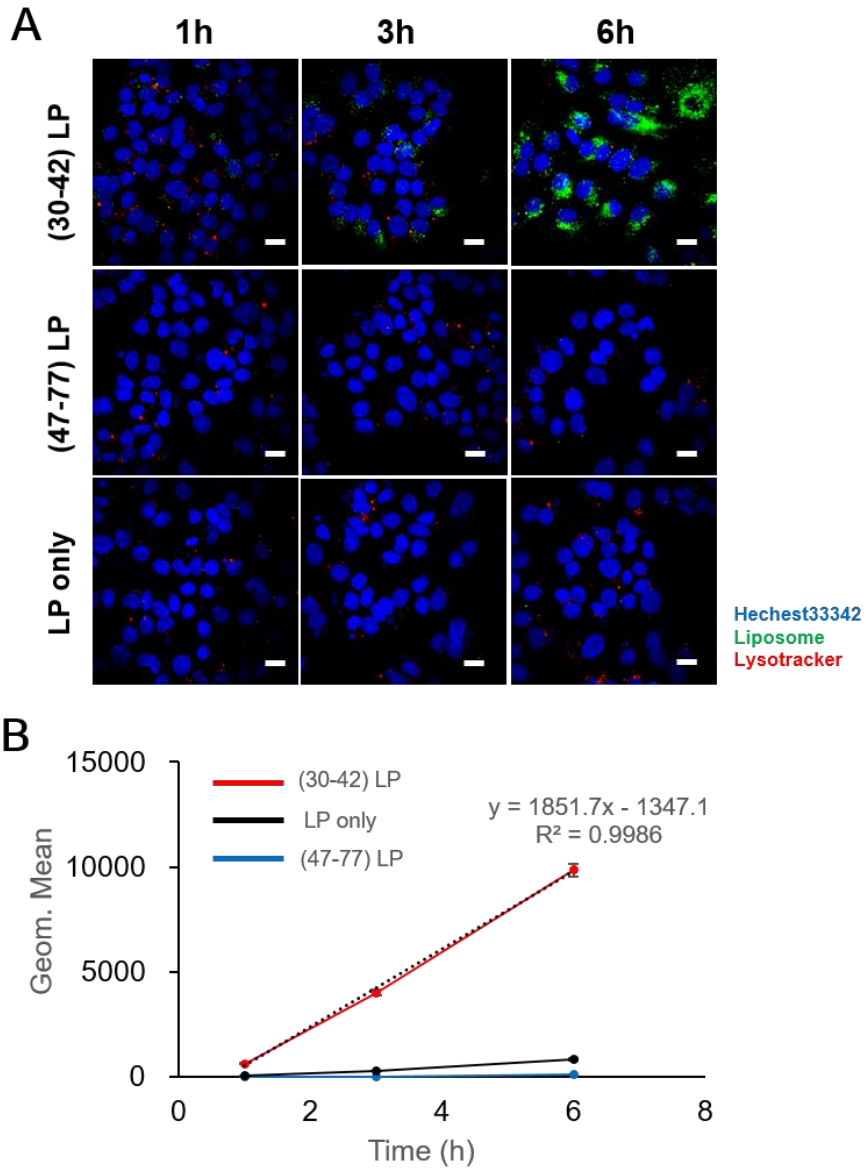

Fig. 14 Time course study of pre-S1 peptide-displaying LPs and unmodified LPs.

Cellular attachment and entry of pre-S1 (30–42)-displaying CellVue-labeled LPs, pre-S1 (47–77)-displaying CellVue-labeled LPs, and CellVue-labeled unmodified LPs in HepG2 cells for 1 h, 3 h, and 6 h. Scale bars represent 20 μm. N=3, error bars represent SDs.

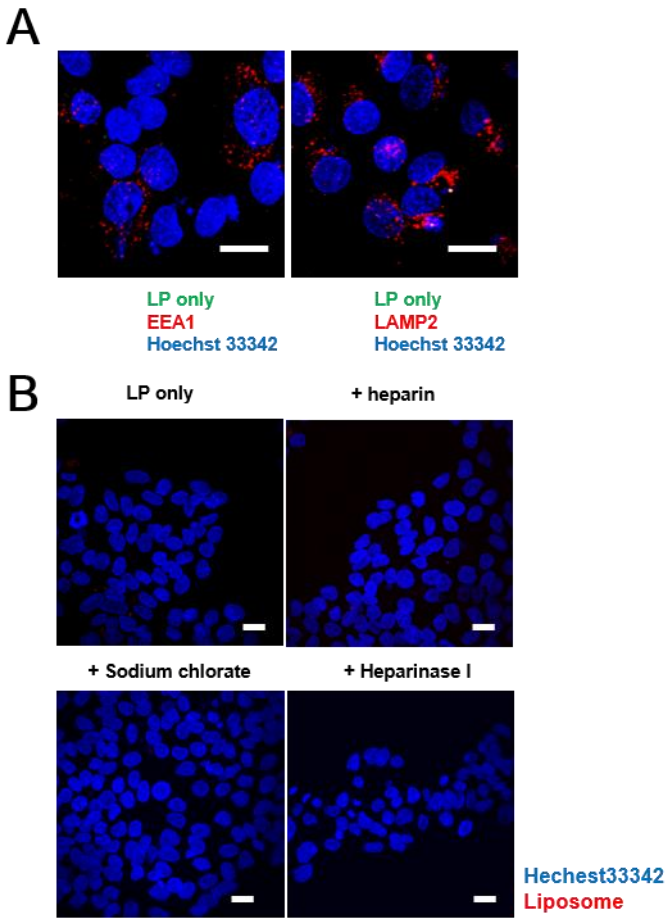

Fig. 15 Intracellular trafficking analyses of unmodified LPs.

Intracellular trafficking analyses of unmodified LPs with/without heparin, Sodium chlorate, and Heparinase I. Scale bars represent 20 μm.

3.3.4. Effect of heparin on the cellular attachment of pre-S1(30–42)-displaying LPs

Because heparin can inhibit the HBV infection efficiently *in vitro* [8], probably by interaction with the pre-S1 region [24, 25], I evaluated the effect of heparin on the cellular attachment of pre-S1(30–42)-displaying LPs. HepG2 cells were pre-treated with heparin sodium salt (from 0.001 to 10 μg/mL) at 37 ℃ for 5 min, and then incubated with

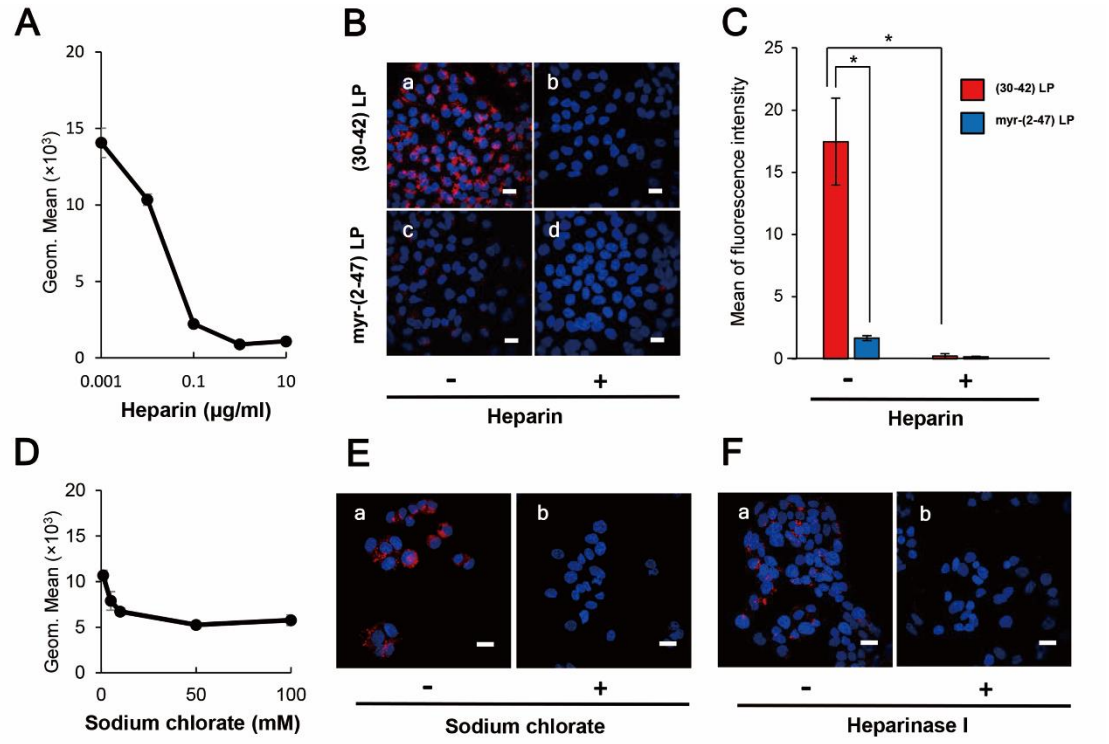

Fig. 16 Effect of cell-surface heparin on the cellular attachment of pre-S1 (30-42)-displaying LPs.

The cellular attachment of pre-S1 (30–42)- and myr-pre-S1 (2–47)-displaying CellVue-labeled LPs on HepG2 cells was analyzed by using Flow cytometry analysis and confocal laser scanning microscope. Treatment with heparin (A, B, and C), sodium chlorate (D and E), and heparinase I (F). Scale bars represent 20 μm. The amounts of fluorophore in each cell were determined using the ImageJ program (B). N=3, error bars represent SDs.

CellVue-labeled pre-S1(30–42)-displaying LPs for 6 h. Under the flow cytometry analysis and LSM observation, heparin was found to inhibit the cellular attachment of pre-S1(30–42)-displaying LPs in a dose-dependent manner, and block the cellular attachment of pre-S1(30–42)- and myr-pre-S1(2–47)-displaying LPs completely at the heparin concentration 10 μg/mL (Fig. 16A, Fig. 16B and Fig. 16C). When HepG2 cells were pre-treated with sodium chlorate (from 1 to 100 mM) for 16h or heparinase I for 1 h, the cellular attachment of CellVue-labeled pre-S1(30–42)-displaying LPs was significantly decreased. (Fig. 16D, Fig. 16E, and Fig. 16F). The effect of heparin on the

cellular uptake of unmodified LPs was evaluated as a control (Fig. 15B). These results strongly suggested that the pre-S1(30–42) region could interact with sulfated glycosaminoglycan chains of cell-surface proteoglycans, which may be involved in the initial cellular attachment of various viruses (*e.g.*, HBV [25], HIV [30], dengue virus [31], adeno-associated virus [32], and herpes simplex virus [33]).

3.3.5. Delineation of the heparin-binding site in pre-S1 region

Pre-S1-derived peptides were displayed on DiD-labeled LPs and mixed with Heparin Sepharose 6 beads. After extensive washing, the fluorophores were eluted with Triton X-100 and quantitated using a fluorescence microplate reader. As shown in Fig. 17A, both pre-S1(30–42)- and myr-pre-S1(2–47)-displaying LPs exhibited a significantly higher affinity to the beads. Furthermore, pre-S1(9–24)-displaying LPs exhibited medium affinity, with a comparable level of LPs displaying conventional heparin-binding peptide from HIV gp120 [34] and vitronectin [35], whereas pre-S1(47–77)-displaying LPs did not exhibit any affinity. Because the affinity of all peptides was nearly lost with a large excess of heparin, these data indicated that the N-terminal half of the pre-S1 region (*i.e.*, from Gly2 to Val47) displays heparin-binding activity and that the pre-S1(30–42) region plays a pivotal role in direct binding with heparin. Next, the LPs displaying three mutated pre-S1(30–42) peptides were subjected to the heparin-binding assay using Heparin Sepharose 6 beads (Fig. 17B). When Trp-32, Phe-34, and Trp-41 were substituted with Ala (pre-S1(30–42, WFW/AAA) peptide), the heparin-binding activity of these LPs decreased significantly (Fig. 17C). The evolutionarily conserved amino acids of the peptide (Asp-31, Trp-32, and Asp-33; pre-S1(30–42, DWD/AAA) peptide) were substituted with Ala, and the heparin-binding activity of the LPs was completely lost,

whereas the peptide harboring mutations at Pro-30, Pro-36, and Pro-42 (pre-S1(30–42, PPP/AAA) peptide) resulted in no significant change in activity. These results strongly suggested that the essential residues for heparin-binding activity are Asp-31, Trp-32, and

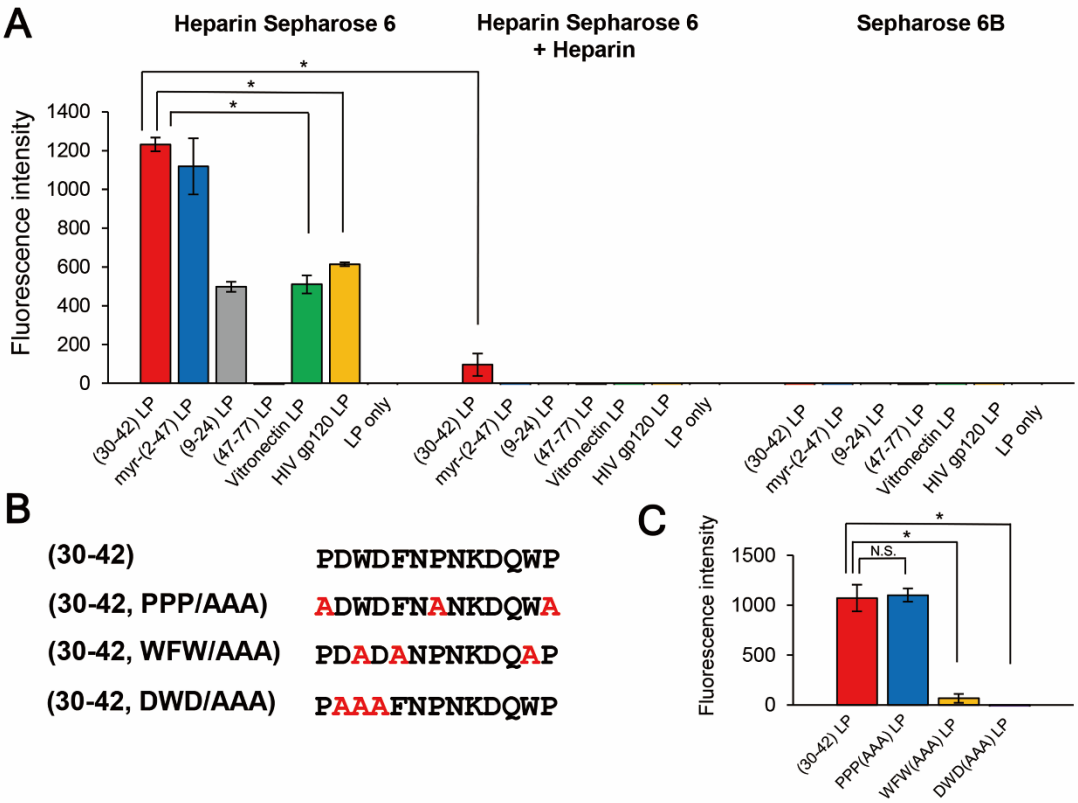

Fig. 17 Direct binding of pre-S1 (30-42)-displaying LPs to heparin.

Pre-S1-derived peptide-displaying DiD-labeled LPs (A) and mutated pre-S1-derived peptide-displaying DiD-labeled LPs (B, C) were incubated with Heparin Sepharose 6. The fluorophores derived from bound LPs were quantitated using a fluorescence microplate reader. Conventional heparin-binding peptides (vitronectin and HIV gp120) were used as controls. N=3, error bars represent SDs.

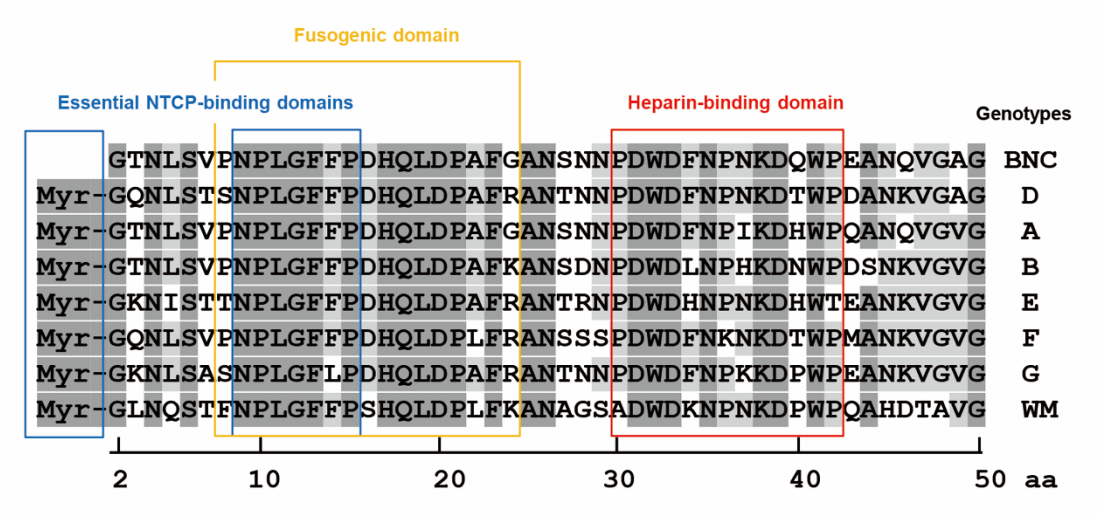

Fig. 18 Comparison of the N-terminal pre-S1 region of various HBV genotypes.

Essential NTCP-binding domains (blue boxes), fusogenic domain (yellow box), and heparin-binding domain (red box). Dark gray highlights indicate well-conserved amino acids, and light gray highlights indicate slightly conserved amino acids.

Asp-33. It is interesting that these amino acids have been well conserved during HBV evolution (Fig. 18).

3.3.6. Cell specificity of the pre-S1(30–42)-displaying LPs

The pre-S1(30–42)-displaying LPs were shown to be promising HBV-mimicking nanocarriers because they could efficiently attach to HepG2 cells in a heparin-dependent manner and then promptly enter the cells via the endocytic pathway (Fig. 13 and Fig. 16). I therefore incubated CellVue-labeled pre-S1(30–42)-displaying LPs with various cells at 37 ℃ for 6 h and analyzed cell specificity by flow cytometry. As shown in Fig. 19A, the pre-S1(30–42)-displaying LPs exhibited higher cellular attachment activity to human hepatic cells (HepG2, primary hepatocyte, Huh7, and NuE cells), human liver endothelial cells Sk-Hep-1, and low activity to rat hepatic MH1C1 cells. No significant activity was observed with human non-hepatic cells (HeLa, A549, HEK293,

and WiDr cells). The myr-pre-S1(2–47)-displaying LPs exhibited lower activity to human hepatic cells than pre-S1(30–42)-displaying LPs (Fig. 19B). Furthermore, the pre-S1(47–77)-displaying LPs could not attach to any of the cells examined (Fig. 19C). Notably, under the same conditions, the LPs displaying conventional heparin-binding peptides (vitronectin and HIV gp120) exhibited broad cellular attachment activity to various cells, including human non-hepatic cells (HeLa, A549, and HEK293, Fig. 19D and 19E). These

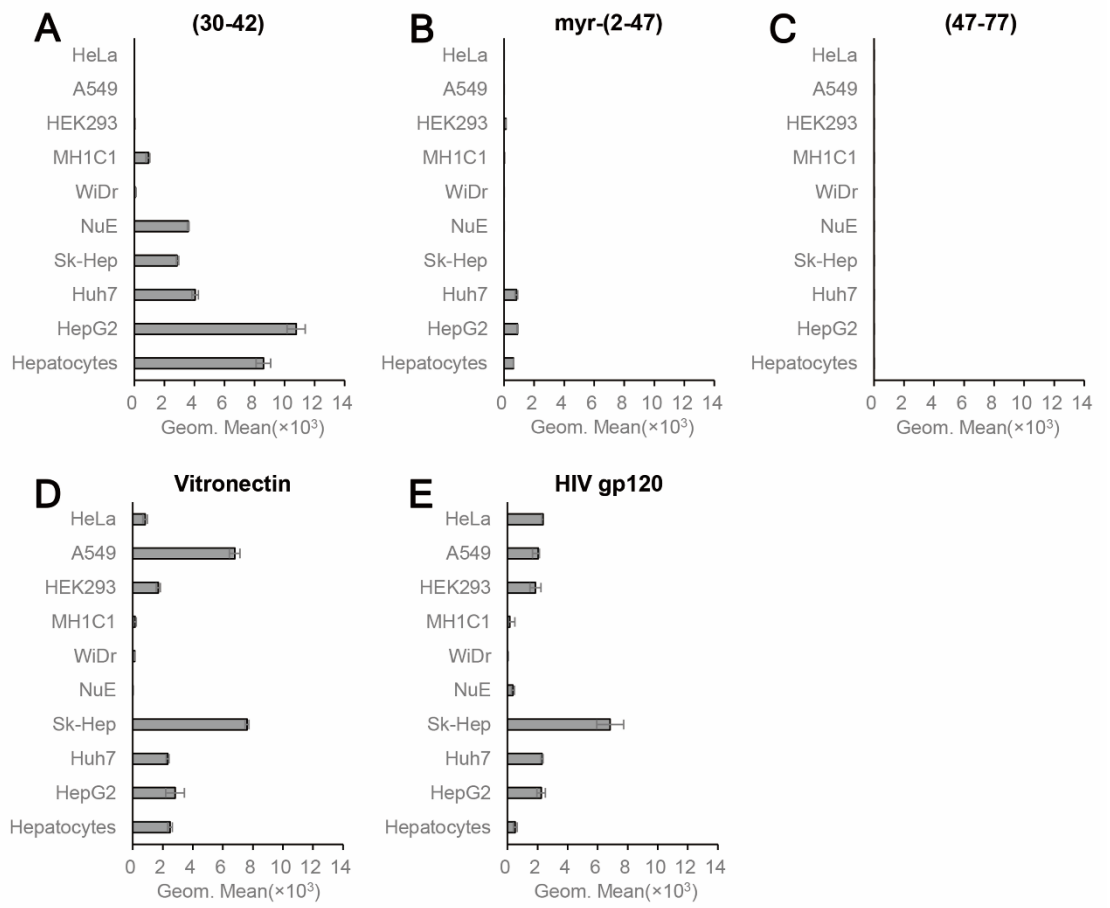

Fig. 19 Cell specificity of pre-S1 (30-42)-displaying LPs.

Pre-S1-derived peptide-displaying CellVue-labeled LPs (A, pre-S1(30–42); B, myr-pre-S1(2–47); C, pre-S1(47–77)) were incubated with various cells, and then analyzed by flow cytometry. Conventional heparin-binding peptides (D, vitronectin; E, HIV gp120) were used as controls. N=3, error bars represent SDs.

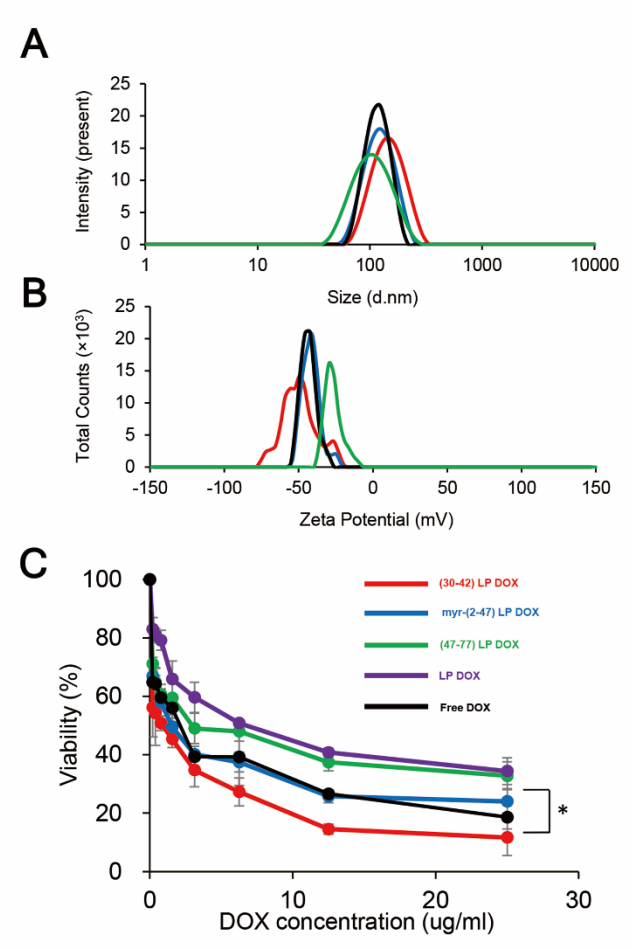

Fig. 20 Cytotoxicity of pre-S1 (30-42)-displaying DOX-containing LPs.

The size (A) and zeta potential (B) of pre-S1-derived peptide-displaying LPs are shown. Pre-S1 (30–42) peptide, red; myr-pre-S1 (2–47) peptide, blue; LP only, green; pre-S1 (47–77) peptide, black. Cytotoxicity of pre-S1-derived peptide-displaying DOX-containing LPs to HepG2 cells (C). Pre-S1 (30–42) peptide, red; myr-pre-S1 (2–47) peptide, blue; pre-S1 (47–77) peptide, green; LP only, purple; and free DOX, black. N=3, error bars represent SDs. Student's t-test; *, $p < 0.005$.

data indicated that the pre-S1(30–42) peptide preferentially interacts with human hepatic cells. Thus, the pre-S1(30–42)-displaying LPs can be used as human hepatic cell-specific HBV-mimicking nanocarriers.

3.3.7. Effect of pre-S1(30-42) peptide on the cytotoxicity of DOX-containing LPs

DOX-containing LPs were modified with the pre-S1(30–42) peptide, myr-pre-S1(2-47) peptide, and pre-S1(47-77) peptide, and incubated with HepG2 cells for an assessment of cytotoxicity. The sizes and ζ-potentials of peptides-displaying LPs containing DOX were shown in Fig. 20A and Fig. 20B, respectively. The efficiency of DOX incorporation of pre-S1(30–42)-displaying LPs, myr-pre-S1(2-47)-displaying LPs, pre-S1(47-77)-displaying LPs, and LPs were estimated to be 93.9% ± 0.28%, 92.8% ± 0.52%, 88.4% ± 0.51%, and 94.0% ± 1.10% (mean ± SD, n=3), respectively. As shown in Fig.20C, pre-S1(30–42)-displaying LPs exhibited the highest cytotoxicity among all samples. The IC_{50} value (50% inhibitory concentration for cell viability) of each sample was ~0.8 μg/mL (pre-S1(30–42)-displaying LPs), ~1.5 μg/mL (myr-pre-S1(2–47)-displaying LPs), ~6.0 μg/mL (pre-S1(47–77)-displaying LPs), ~6.2 μg/mL (LPs alone), and ~1.5 μg/mL (free DOX). Furthermore, the intracellular distribution of DOX after the treatment was shown in Fig 21. The intracellular DOX was mainly localized in the nuclei. No cytotoxicity was found in pre-S1(30–42)-displaying LPs without DOX (Fig. 22). These results indicated that the pre-S1(30–42) peptide, rather than other peptides, can enhance the efficient cellular uptake of DOX-containing LPs by HepG2 cells.

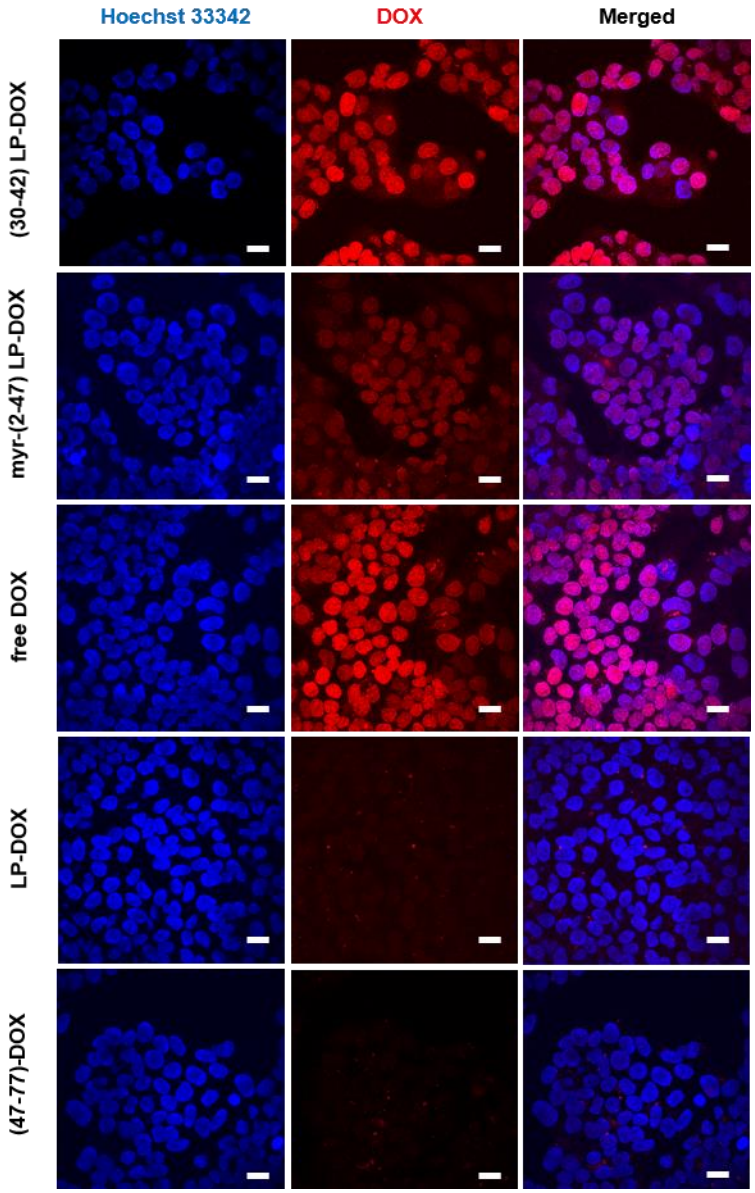

Fig. 21 Intracellular distribution of doxorubicin by peptide-displaying LPs.

Scale bars represent 20 μm.

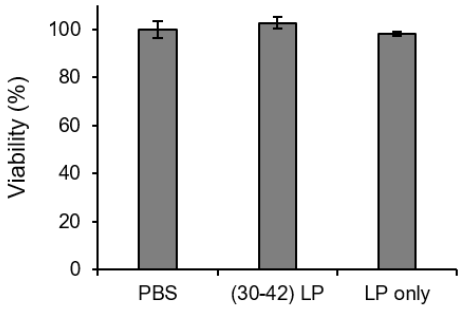

Fig. 22 Cytotoxicity analyses of peptide-displaying LPs and unmodified LPs without DOX.

N=3, error bars represent SDs.

3.4. Discussion

HBV was recently proposed to interact with HSPG as a primary receptor [8, 25] and subsequently be transferred to NTCP as a secondary receptor for the establishment of infection [10, 36]. The key viral determinant of HBV infection is the N-terminal myristoylated pre-S1(2–47) domain, because the associated peptide can block HBV infection by inhibiting NTCP-dependent cell entry [10]. However, cell-surface NTCP is not involved in the initial cellular attachment of HBV [23]; rather, the HSPG-interacting domain is important in the early infection machinery of HBV. For a long time, there has been controversy about whether the HSPG-interacting domain is located in the pre-S region [25] or S region [37-39]. Recently, HBV virions were revealed to change their morphology in the bloodstream from an N-type virion to a B-type virion, and then to acquire infectivity to human hepatic cells [24]. The N-type virion, which hides the pre-S region in its interior cavity, cannot bind to HSPG and primary human hepatocytes, whereas the B-type virion, which exposes the pre-S region to its exterior space, can bind to HSPG and primary human hepatocytes to establish infection. Because both N and B virion types expose the S region to its exterior space, the pre-S region might be a key determinant for interaction with HSPG. Our results indicated that the N-terminal half of the pre-S1 region (from Asn-9 to Val-47) can interact with HSPG (Fig. 7 and Fig. 16). The pre-S1(30–42) domain, particularly, plays a pivotal role in interactions with HSPG, and evolutionarily conserved residues (Asp-31, Trp-32, and Asp-33) are indispensable for this interaction (Fig. 17). Another research group reported that neutralizing antibody KR127 directly interacted with the pre-S1(26–34) region [40], suggesting that the KR127 antibody inhibits HBV infection by restricting the function of the evolutionarily conserved amino acids (Asp-31, Trp-32, and Asp-33). N-terminal pre-S1-derived

peptides, especially myr-pre-S1(2-48) peptide [41-43] and myr-pre-S1(2-47) peptide [10], have been revealed to inhibit HBV infection efficiently. In an *in vitro* HBV infection assay, the myr-pre-S1(2–18) peptide inhibited HBV infection of *Tupaia* hepatocytes, whereas neither the myr-pre-S1(2–8) nor myr-pre-S1(19–48) peptides block the HBV infection these cells [41]. Notably, the myr-pre-S1(2–48) peptide showed highest inhibition activity. Furthermore, point mutations between Asn-9 and Phe-14 in the myr-pre-S1(2–48) peptide abrogated its inhibition of HBV infection [10, 43]. These results indicated that the myr-pre-S1(9–18) region is essential for HBV infection (presumably by acting as an essential NTCP-binding domain; see Fig. 18) and that the pre-S1(19–48) region supports the function of the myr-pre-S1(9–18) region. Therefore, the pre-S1(30–42) domain may be a key determinant in the enhancement of HBV infection.

Generally, cell entry by viruses is executed through complicated steps, including receptor attachment, endocytosis, membrane fusion, and endosomal escape. Interestingly, the evolutionarily conserved residues in the pre-S1(9–47) region harbor many functional domains (Fig. 18), including the essential NTCP-binding domain (N-terminal myristoylation, from Asn-9 to Pro-15), low pH-dependent fusogenic domain (from Asn-9 to Gly-24), and heparin-binding domain (from Pro-30 to Pro-42). Recently, by using a targeted RNA interference screening, glypican 5, a family of glycosylphosphatidylinositol-anchored HSPG, was found to be one of the initial attachment receptors for HBV [44]. These data have led us to propose a new model of HBV early infection: initial attachment of the pre-S1(30–42) region to cell-surface HSPG, cell entry by endocytosis, interactions of myristoyl residues and the pre-S1(9–15) region with endosomal NTCP, exposure of the pre-S1 (9–24) region through a conformational change in the L protein, induction of full membrane fusion between the HBV membrane

and endosomal membrane under acidic conditions, and then escape of the virus core from late endosomes.

HSPG is widely utilized as an initial cell attachment receptor for various viruses and nanocarriers, including hepatitis C virus [45], porcine circovirus 2 [46], herpes simplex virus [33], exosomes [47], apolipoprotein E-derived peptide-modified LPs [48], and cell-penetrating peptide-modified LPs [49], because HSPG is ubiquitously expressed in various tissues [35]. Many heparin-binding peptides have been identified in viral and heparin-binding proteins that can interact with various types of cells. It is noteworthy that hepatitis C virus could infect hepatic cells specifically by the help of highly sulfated glycosaminoglycans (GAGs) found in liver [45, 50]. The liver-specific infection of HBV could be blocked by heparin or other highly sulfated GAGs, but not by lower sulfated GAG [8]. These studies suggested that highly sulfated GAGs specifically expressed in liver may be responsible for the liver-specific uptake of HBV.

In this study, I identified a novel heparin-binding peptide, pre-S1(30–42), that shows a strong affinity for human hepatic cells (Fig. 19). The surface charges of conventional heparin-binding peptides are often positive. The theoretical isoelectric points of heparin-binding peptides of HIV gp120, vitronectin, adeno-associated virus 2 VP3, equine arteritis virus E protein, and eastern equine encephalitis virus E2 glycoprotein are 12.48, 12.48, 12.00, 11.83, and 10.30, respectively [51-56], whereas that of the pre-S1(30–42) peptide is 3.93. I postulated that the pre-S1(30–42) peptide, especially the hydrophobic segment consisting of Asp-31, Trp-32, and Asp-33, interacts with heparin through hydrophobic interactions rather than electrostatic interactions. Because highly sulfated heparin is commonly found in human hepatic cells [50] and treatment with sodium chlorate abrogated the interactions between pre-S1(30–42)-

displaying LPs and sulfated glycosaminoglycan chains (Fig. 16), thus, as described above, the strong affinity of the pre-S1(30–42) peptide to human hepatic cells may be sustained by the highly sulfated residues in HSPG. Although the cellular uptake of pre-S1(30–42)-displaying LPs was significantly higher than that of myr-pre-S1(2–47)-displaying LPs (Fig 7B and Fig. 10B), the binding affinity to heparin Sepharose 6 of these LPs was similar (Fig. 17A). Unlike pre-S1(30-42) peptide, myr-pre-S1(2-47) peptide contains two membrane-interacting domains, N-terminal myristoyl group and fusogenic domain pre-S1(9-24) [20]. It was suggested that these domains may hamper the cellular entry of myr-pre-S1(2-47)-displaying LPs by interacting with plasma membrane.

The pre-S1(30-42) peptide shows negative charge in physiological conditions, while conventional heparin-binding peptides exhibit positive charge. Owing to this unique property, pre-S1(30-42)-displaying nanocarriers are expected to show reduced non-specific interaction with biomolecules and cells during blood circulation. Especially, macrophages prefer to engulf positively charged materials more efficiently than negatively charged ones [57]. Collectively, the stringent hepatotrophic property of HBV is mediated by two domains residing in the myr-pre-S1(2–47) region. The pre-S1(30–42) region first interacts with highly sulfated heparin on human hepatic cells. After HSPG-mediated endocytosis, the myr-pre-S1(9–15) region interacts with NTCP in endosomes. This working hypothesis agrees well with the present model for the mechanism underlying HBV early infection [23, 58].

3.5. Conclusions

I identified a novel heparin-binding domain in the N-terminal half of the pre-S1 region (from Pro-30 to Pro-42), localized close to the low-pH fusogenic domain (from

Asn-9 to Gly-24) and NTCP-binding site (N-terminal myristoyl residue and from Asn-9 to Pro-15). The pre-S1(30–42) peptide showed higher specificity for human hepatic cell-derived heparin, and the evolutionarily conserved residues Asp-31, Trp-32, and Asp-33 were found to indispensable for this activity. Our results shed light on the early infection machinery of HBV, elucidating how functional domains in the myr-pre-S1(2–42) region are coordinated on a molecular basis. Finally, since the pre-S1(30–42) domain is involved in the initial cellular attachment of HBV, pre-S1(30–42)-displaying LPs can be used as efficient human hepatic cell-specific HBV-mimicking DDS nanocarriers.

References

1. M.J. Ernsting, M. Murakami, A. Roy, S.D. Li, Factors controlling the pharmacokinetics, biodistribution and intratumoral penetration of nanoparticles, *Journal of Controlled Release*, 2013, 172, 782-794.
2. L.C. Davies, S.J. Jenkins, J.E. Allen, P.R. Taylor, Tissue-resident macrophages, *Nature Immunology*, 2013, 14, 986-995.
3. R. Singh, J.W. Lillard, Jr., Nanoparticle-based targeted drug delivery, *Experimental and Molecular Pathology*, 2009, 86, 215-223.
4. B. Yameen, W.I. Choi, C. Vilos, A. Swami, J. Shi, O.C. Farokhzad, Insight into nanoparticle cellular uptake and intracellular targeting, *Journal of Controlled Release*, 2014, 190, 485-499.
5. T.M. Allen, P.R. Cullis, Drug delivery systems: entering the mainstream, *Science*, 2014, 303, 1818-1822.
6. H. Yin, R.L. Kanasty, A.A. Eltoukhy, A.J. Vegas, J.R. Dorkin, D.G. Anderson, Non-viral vectors for gene-based therapy, *Nature Reviews. Genetics*, 2014, 15, 541-555.

7. P. Tiollais, C. Pourcel, A. Dejean, The hepatitis B virus, *Nature*, 1985, 317, 489-495.
8. C.M. Leistner, S. Gruen-Bernhard, D. Glebe, Role of glycosaminoglycans for binding and infection of hepatitis B virus, *Cellular Microbiology*, 2008, 10, 122-133.
9. O. Lamas Longarela, T.T. Schmidt, K. Schoneweis, R. Romeo, H. Wedemeyer, S. Urban, A. Schulze, Proteoglycans act as cellular hepatitis delta virus attachment receptors, *PloS One*, 2013, 3, e58340.
10. H. Yan, G. Zhong, G. Xu, W. He, Z. Jing, Z. Gao, Y. Huang, Y. Qi, B. Peng, H. Wang, L. Fu, M. Song, P. Chen, W. Gao, B. Ren, Y. Sun, T. Cai, X. Feng, J. Sui, W. Li, Sodium taurocholate cotransporting polypeptide is a functional receptor for human hepatitis B and D virus, *eLife*, 2012, 1, e00049.
11. H.C. Huang, C.C. Chen, W.C. Chang, M.H. Tao, C. Huang, Entry of hepatitis B virus into immortalized human primary hepatocytes by clathrin-dependent endocytosis, *Journal of Virology*, 2012, 86, 9443-9453.
12. S. Kuroda, S. Otaka, T.Miyazaki, M. Nakao, Y. Fujisawa, Hepatitis B virus envelope L protein particles: synthesis and assembly in Saccharomyces cerevisiae, purification and characterization, *Journal of Biological Chemistry*, 1992, 267, 1953–1961.
13. M. Somiya, Q. Liu, S. Kuroda, Current progress of virus-mimicking nanocarriers for drug delivery, *Nanotheranostics*, 2017, 1, 415-429.
14. T. Yamada, Y. Iwasaki, H. Tada, H. Iwabuki, M.K.L. Chuah, T. VandenDriessche, H. Fukuda, A. Kondo, M. Ueda, M. Seno, K. Tanizawa, S. Kuroda, Nanoparticles for the delivery of genes and drugs to human hepatocytes, *Nature Biotechnology*, 2003, 21, 885–890.

15. J. Jung, T. Matsuzaki, K. Tatematsu, T. Okajima, K. Tanizawa, S. Kuroda, Bio-nanocapsule conjugated with liposomes for in vivo pinpoint delivery of various materials, *Journal of Controlled Release*, 2008, 126, 255-264.
16. T. Kasuya, J. Jung, R. Kinoshita, Y. Goh, T. Matsuzaki, M. Iijima, N. Yoshimoto, K. Tanizawa, S.i. Kuroda, Bio-nanocapsule–liposome conjugates for in vivo pinpoint drug and gene delivery, *Methods in Enzymology*, 2009, 464, 147-166.
17. Q. Liu, J. Jung, M. Somiya, M. Iijima, N. Yoshimoto, T. Niimi, A.D. Maturana, S.H. Shin, S.Y. Jeong, E.K. Choi, S. Kuroda, Virosomes of hepatitis B virus envelope L proteins containing doxorubicin: synergistic enhancement of human liver-specific antitumor growth activity by radiotherapy, *International Journal of Nanomedicine*, 2015, 10, 4159-4172.
18. Y. Itoh, S. Kuroda, T. Miyazaki, S. Otaka, Y. Fujisawa, Identification of polymerized-albumin receptor domain in the pre-S2 region of hepatitis B virus surface antigen M protein, *Journal of Biotechnology*, 1992, 23, 71-82.
19. A.R. Neurath, S.B. Kent, N. Strick, K. Parker, Identification and chemical synthesis of a host cell receptor binding site on hepatitis B virus, *Cell*, 1986, 46, 429–436.
20. M. Somiya, Y. Sasaki, T. Matsuzaki, Q. Liu, M. Iijima, N. Yoshimoto, T. Niimi, A.D. Maturana, S. Kuroda, Intracellular trafficking of bio-nanocapsule-liposome complex: Identification of fusogenic activity in the pre-S1 region of hepatitis B virus surface antigen L protein, *Journal of Controlled Release*, 2015, 212, 10-18.
21. Q. Liu, M. Somiya, N. Shimada, W. Sakamoto, N. Yoshimoto, M. Iijima, K. Tatematsu, T. Nakai, T. Okajima, A. Maruyama, S. Kuroda, Mutational analysis of hepatitis B virus pre-S1 (9-24) fusogenic peptide, *Biochemical and Biophysical Research Communications*, 2016, 474, 406-412.

22. X. Zhang, Q. Zhang, Q. Peng, J. Zhou, L. Liao, X. Sun, L. Zhang, T. Gong, Hepatitis B virus preS1-derived lipopeptide functionalized liposomes for targeting of hepatic cells, *Biomaterials*, 2014, 35, 6130-6141.

23. M. Somiya, Q. Liu, N. Yoshimoto, M. Iijima, K. Tatematsu, T. Nakai, T. Okajima, K. Kuroki, K. Ueda, S. Kuroda, Cellular uptake of hepatitis B virus envelope L particles is independent of sodium taurocholate cotransporting polypeptide, but dependent on heparan sulfate proteoglycan, *Virology*, 2016, 497, 23-32.

24. S. Seitz, C. Iancu, T. Volz, W. Mier, M. Dandri, S. Urban, R. Bartenschlager, A slow maturation process renders hepatitis B virus infectious, *Cell Host & Microbe*, 2016, 20, 25-35.

25. A. Schulze, P. Gripon, S. Urban, Hepatitis B virus infection initiates with a large surface protein-dependent binding to heparan sulfate proteoglycans, *Hepatology*, 2007, 46, 1759-1768.

26. A. Fritze, F. Hens, A. Kimpfler, R. Schubert, R. Peschka-Suss, Remote loading of doxorubicin into liposomes driven by a transmembrane phosphate gradient, *Biochimica et Biophysica Acta*, 2006, 1758, 1633-1640.

27. M. Yamada, A. Oeda, J. Jung, M. Iijima, N. Yoshimoto, T. Niimi, S.Y. Jeong, E.K. Choi, K. Tanizawa, S. Kuroda, Hepatitis B virus envelope L protein-derived bio-nanocapsules: mechanisms of cellular attachment and entry into human hepatic cells, *Journal of Controlled Release*, 2012, 160, 322-329.

28. H.C. Huang, C.C. Chen, W.C. Chang, M.H. Tao, C. Huang, Entry of hepatitis B virus into immortalized human primary hepatocytes by clathrin-dependent endocytosis, *Journal of Virology*, 2012, 86, 9443-9453.

29. E. Smythe, G. Warren, The mechanism of receptor-mediated endocytosis, *European Journal of Biochemistry*, 1991, 202, 689-699.

30. L. de Witte, M. Bobardt, U. Chatterji, G. Degeest, G. David, T.B. Geijtenbeek, P. Gallay, Syndecan-3 is a dendritic cell-specific attachment receptor for HIV-1, *Proceedings of the National Academy of Sciences of the United States of America*, 2007, 104, 19464-19469.

31. Y. Chen, T. Maguire, R.E. Hileman, J.R. Fromm, J.D. Esko, R.J. Linhardt, R.M. Marks, Dengue virus infectivity depends on envelope protein binding to target cell heparan sulfate, *Nature Medicine*, 1997, 3, 866-871.

32. J. O'Donnell, K.A. Taylor, M.S. Chapman, Adeno-associated virus-2 and its primary cellular receptor--Cryo-EM structure of a heparin complex, *Virology*, 2009, 385, 434-443.

33. M.T. Shieh, D. WuDunn, R.I. Montgomery, J.D. Esko, P.G. Spear, Cell surface receptors for herpes simplex virus are heparan sulfate proteoglycans, *The Journal of Cell Biology*, 1992, 166, 1273-1281.

34. E. Crublet, J.P. Andrieu, R.R. Vives, H. Lortat-Jacob, The HIV-1 envelope glycoprotein gp120 features four heparan sulfate binding domains, including the co-receptor binding site, *The Journal of Biological Chemistry*, 2008, 283,15193-15200.

35. M. Bernfield, M. Götte, P.W. Park, O. Reizes, M.L. Fitzgerald, J. Lincecum, M. Zako, Functions of cell surface heparan sulfate proteoglycans, *Annual Review of Biochemistry*, 1999, 68, 729-777.

36. Y. Ni, F.A. Lempp, S. Mehrle, S. Nkongolo, C. Kaufman, M. Falth, J. Stindt, C. Koniger, M. Nassal, R. Kubitz, H. Sultmann, S. Urban, Hepatitis B and D viruses

exploit sodium taurocholate co-transporting polypeptide for species-specific entry into hepatocytes, *Gastroenterology*, 2014, 146, 1070-1083.

37. G. Abou-Jaoude, C. Sureau, Entry of hepatitis delta virus requires the conserved cysteine residues of the hepatitis B virus envelope protein antigenic loop and is blocked by inhibitors of thiol-disulfide exchange, *Journal of Virology*, 2007, 81, 13057-13066.
38. J. Salisse, C. Sureau, A function essential to viral entry underlies the hepatitis B virus "a" determinant, *Journal of Virology*, 2009, 83, 9321-9328.
39. C. Sureau, J. Salisse, A conformational heparan sulfate binding site essential to infectivity overlaps with the conserved hepatitis B virus a-determinant, *Hepatology*, 2013, 57, 985-994.
40. H.J. Hong, C.J. Ryu, H. Hur, S. Kim, H.K. Oh, M.S. Oh, S.Y. Park, In vivo neutralization of hepatitis B virus infection by an anti-preS1 humanized antibody in chimpanzees, *Virology*, 2004, 318, 134-141.
41. D. Glebe, S. Urban, E.V. Knoop, N. Çağ, P. Krass, S. Grün, A. Bulavaite, K. Sasnauskas, W.H. Gerlich, Mapping of the hepatitis B virus attachment site by use of infection-inhibiting preS1 lipopeptides and Tupaia hepatocytes, *Gastroenterology*, 2005, 129, 234-245.
42. P. Gripon, I. Cannie, S. Urban, Efficient inhibition of hepatitis B virus infection by acylated peptides derived from the large viral surface protein, *Journal of Virology*, 2005, 79, 1613-1622.
43. M. Engelke, K. Mills, S. Seitz, P. Simon, P. Gripon, M. Schnolzer, S. Urban, Characterization of a hepatitis B and hepatitis delta virus receptor binding site, *Hepatology*, 2006, 43, 750-760.

44. E.R. Verrier, C.C. Colpitts, C. Bach, L. Heydmann, A. Weiss, M. Renaud, S.C. Durand, F. Habersetzer, D. Durantel, G. Abou-Jaoudé, M.M. López Ledesma D.J. Felmlee, M. Soumillon, T. Croonenborghs, N. Pochet, M. Nassal, C. Schuster, L. Brino, C. Sureau, M.B. Zeisel, T.F. Baumert, A targeted functional RNA interference screen uncovers glypican 5 as an entry factor for hepatitis B and D viruses, *Hepatology*, 2016, 63, 35-48.

45. H. Barth, C. Schafer, M.I. Adah, F. Zhang, R.J. Linhardt, H. Toyoda, A. Kinoshita-Toyoda, T. Toida, T.H. Van Kuppevelt, E. Depla, F. Von Weizsacker, H.E. Blum, T.F. Baumert, Cellular binding of hepatitis C virus envelope glycoprotein E2 requires cell surface heparan sulfate, *The Journal of Biological Chemistry*, 2003, 278, 41003-41012.

46. G. Misinzo, P.L. Delputte, P. Meerts, D.J. Lefebvre, H.J. Nauwynck, Porcine circovirus 2 uses heparan sulfate and chondroitin sulfate B glycosaminoglycans as receptors for its attachment to host cells, *Journal of Virology*, 2006, 80, 3487-3494.

47. H.C. Christianson, K.J. Svensson, T.H. van Kuppevelt, J.P. Li, M. Belting, Cancer cell exosomes depend on cell-surface heparin sulfate proteoglycans for their internalization and functional activity, *Proceedings of the National Academy of Sciences of the United States of America*, 2013, 110, 17380-17385.

48. I. Sauer, I.R. Dunay, K. Weisgraber, M. Bienert, M. Dathe, An apolipoprotein E-derived peptide mediates uptake of sterically stabilized liposomes into brain capillary endothelial cells, *Biochemistry*, 2015, 44, 2021-2029.

49. C. Marty, C. Meylan, H. Schott, K. Ballmer-Hofer, R.A. Schwendener, Enhanced heparan sulfate proteoglycan-mediated uptake of cell-penetrating peptide-modified liposomes, *Cellular and Molecular Life Sciences*, 2004, 61, 1785-1794.

50. P. Vongchan, M. Warda, H. Toyoda, T. Toida, R.M. Marks, R.J. Linhardt, Structural characterization of human liver heparan sulfate, *Biochimica et Biophysica Acta*, 2005, 1721, 1-8.

51. B. Bjellqvist, G.J. Hughes, C. Pasquali, N. Paquet, F. Ravier, J.C. Sanchez, S. Frutiger, D.F. Hochstrasser, The focusing positions of polypeptides in immobilized pH gradients can be predicted from their amino acid sequences. *Electrophoresis*, 1993, 14, 1023-1031.

52. B. Bjellqvist, B. Basse, E. Olsen, J.E. Celis, Reference points for comparisons of two-dimensional maps of proteins from different human cell types defined in a pH scale where isoelectric points correlate with polypeptide compositions. *Electrophoresis*, 1994, 15, 529-539.

53. E. Gasteiger, C. Hoogland, A. Gattiker, S. Duvaud, M.R. Wilkins, R.D. Appel, A. Bairoch, Protein Identification and Analysis Tools on the ExPASy Server, *Methods in Molecular Biology*, 1999, 112, 531-552.

54. A. Kern, K. Schmidt, C. Leder, O.J. Muller, C.E. Wobus, K. Bettinger, C.W. Von der Lieth, J.A. King, J.A. Kleinschmidt, Identification of a heparin-binding motif on adeno-associated virus type 2 capsids, *Journal of Virology*, 2003, 77, 11072-11081.

55. Z. Lu, S. Sarkar, J. Zhang, U.B. Balasuriya, Conserved arginine residues in the carboxyl terminus of the equine arteritis virus E protein may play a role in heparin binding but may not affect viral infectivity in equine endothelial cells, *Archives of Virology*, 2016, 161, 873-886.

56. C.L. Gardner, J. Choi-Nurvitadhi, C. Sun, A. Bayer, J. Hritz, K.D. Ryman, W.B. Klimstra, Natural variation in the heparan sulfate binding domain of the eastern

equine encephalitis virus E2 glycoprotein alters interactions with cell surfaces and virulence in mice, *Journal of Virology*, 2013, 87, 8582-8590.

57. Y. Tabata, Y Ikada. Effect of the size and surface charge of polymer microspheres on their phagocytosis by macrophage. *Biomaterials*, 1988, 9, 256-362

58. S. Urban, R. Bartenschlager, R. Kubitz, F. Zoulim, Strategies to inhibit entry of HBV and HDV into hepatocytes, *Gastroenterology*, 2014, 147, 48-64.

Chapter IV

Comprehensive Discussion

Drug delivery system (DDS) nanocarrier is a state of art technology for therapeutic agents (*i.e.*, chemical compounds, proteins, and genes) to maximize efficacy and minimize undesirable side effects [1]. Nanomaterials, including liposomes (LPs), polymers, lipid-like nanoparticles (LNPs), nanogels, micelles, and viral vectors [2] have been widely used as DDS nanocarriers for encapsulating agents, which could enhance drug solubility, optimize half-life in bloodstream, increase drug concentrations in diseased tissues, and reduce the damage to normal tissues on extravasation [1-3]. The development of DDS nanocarriers has so far been based on a "trial and error" process of material composition, encapsulation method, physiological parameter optimization (*i.e.*, nanoparticle size, shape, zeta potential, and stability), safety test, and therapeutic efficacy evaluation [4]. At present, non-viral DDS nanocarriers such as LPs, LNPs, and nanomicelles are widely used in basic research and clinical trials, due to its high safety, high drug encapsulation efficiency, low immunogenicity, and simple CMC (chemistry, manufacturing, and controls) [5]. While these nanocarriers were modified with functional moieties for targeting, cell penetrating, and immune evasion, they have not yet exhibited sufficient abilities of *in vivo* targeting, cell attachment, cell entry, endosomal escape, and drug release concurrently. On the other hand, viral DDS nanocarriers such as adenoviruses, adeno-associated viruses, lentiviruses possess the aforementioned abilities sufficiently, whereas several issues such as pathogenicity, immunogenicity, and complicated CMC should be addressed for expanding the range of their applications [5]. Thus, the hybrid materials harboring the advantages of viral and non-viral DDS nanocarriers have been expected as promising DDS nanocarriers for a long time [6].

Our group have developed a candidate of hybrid DDS nanocarriers by using approximately 50-nm HBV envelope L protein particle, synthesized in *Saccharomyces cerevisiae* (named as a bio-nanocapsule (BNC))[7]. Since BNC consists of complete envelope protein and excludes HBV-derived pathogenic components (*i.e.*, genome, core antigens) and shares similar structure with an immunogen of conventional HB vaccines, it is considered that BNC is a safe material equipped with HBV early infection machinery. When encapsulated chemical compounds, proteins, and genes into BNC by electroporation, they could deliver payloads specifically and efficiently to human hepatic cells *in vitro* and *in vivo* [8]. Furthermore, BNC could fuse with LPs leading to the formation of BNC-LP complexes under the neutral conditions [9, 10] or virosomes under high temperature and acidic conditions [11]. Both BNC-LP complexes and virosomes could exhibit higher drug/gene loading capability and deliver payloads to human hepatic cells more efficiently and specifically [9-11]. Moreover, our group developed low immunogenic BNC by mimicking HBV escape mutants [12] and identified the polymerized albumin receptor in pre-S2 region as an immune evasion domain [6]. Although BNC has been successfully demonstrated as a promising hybrid DDS nanocarrier, the complicated CMC caused by the nature of biologics have hampered the expansion of its application range.

For overcoming the CMC-related disadvantage of BNC, I focused on the functional domains in L protein indispensable for the early infection machinery of HBV, and tried to reconstitute the machinery on the surface of non-viral DDS nanocarriers (Fig.

23). The early infection machinery of HBV consists of four processes, such as cell attachment, cell entry, endosomal escape, and uncoating. However, each process has not been fully elucidated on the molecular basis (see Fig. 2): how HBV interacts with HSPG initially on the surface of target cell, how HBV transfers from HSPG to NTCP in

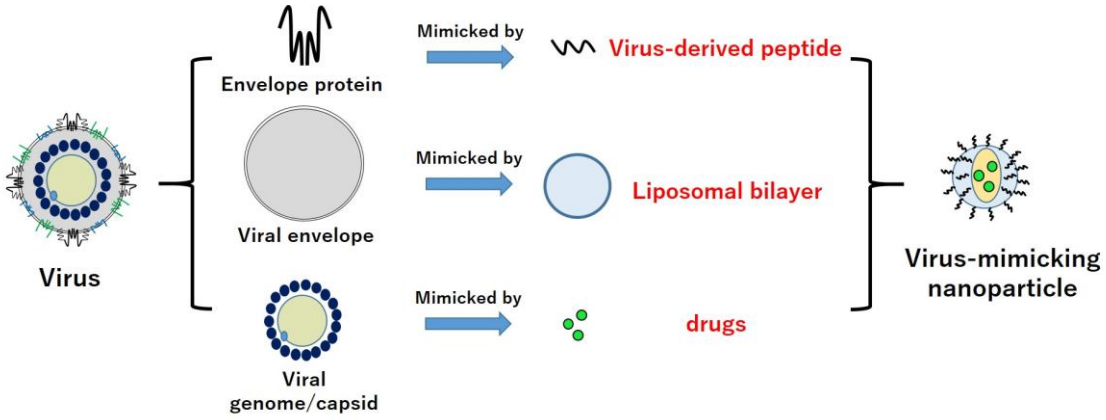

Fig. 23 Schematic of virus-mimicking nanoparticle.

endosomes, and how NTCP is involved in the endosomal escape and uncoating process of HBV.

In this thesis, I analyzed the molecular mechanism underlying membrane disruption/fusion activity of pre-S1(9-24) and identified a novel heparin-binding domain pre-S1(30-42). Both domains might play pivotal roles in the HBV early infection machinery and could contribute to the establishment of efficient HBV-mimicking DDS nanocarriers. However, it is necessary for the forthcoming DDS nanocarriers to harbor defined mechanisms for their cell entry and endosome escape [1, 2]. Recently, various membrane disruption/fusion peptides have been installed to DDS nanocarriers for enhancing the endosomal escape of encapsulated drugs (e.g., HIV-derived transactivator of transcription (tat) peptide [13]). Generally, these peptides exhibit either highly positive charge or hydrophobic property, hampering the modification with other functional

moieties for targeting and immune evasion onto the surface of nanoparticles [4]. Basic amino acids, Arg or Lys, could contribute to the membrane attachment, the hole formation, and thereby the disruption of membrane structure [13, 14]. However, when the strong electrostatic interaction occurs between basic amino acids and plasma membrane, the cells would be severely damaged by an unwanted cellular cytotoxicity. Thus, the membrane disruption/fusion peptides for DDS nanocarriers should be tuned precisely not to show severe cytotoxicity in the endosomes under acidic conditions. Viruses are naturally occurring DDS nanocarriers, which exhibit sophisticated endosomal escape without showing strong cytotoxicity in their early infection machineries [15]. The use of virus-derived fusogenic peptides is one of the most plausible strategy for development of the forthcoming DDS nanocarriers. In Chapter II, I analyzed the membrane disruption/fusion mechanism of HBV-derived pre-S1(9-24) by using mutated peptide-displaying LPs. Finally, I found that the low pH-dependent membrane disruption/fusion activity is well correlated with the hydrophobicity of pre-S1(9-24), especially the hydrophobic clusters located at both ends. Two acidic amino acids, Asp-16 and Asp-20, act as sensing acidic conditions to induce the membrane fusion, which is the similar function to the Glu-15 and Asp-19 of the fusogenic domain of influenza virus hemagglutinin protein [16]. Generally, virus-derived fusogenic peptides harbor rigid structures (α-helix or β-sheet) under acidic conditions for facilitating the membrane interaction. However, the pre-S1(9-24) fusogenic domain exhibited a random-coil structure even under acidic conditions, which has been found only in the flavivirus envelope protein-derived fusogenic peptide [17]. It remains unclear how the fusogenic peptides of HBV and flavivirus function for membrane fusion on the molecular basis.

In Chapter III, I identified two heparin-binding domains in the pre-S1 region, pre-S1(9-24) with weak affinity and pre-S1(30-42) with strong affinity (see Fig. 17). To my knowledge, it is infrequent that such a short region contains multiple functional domains, namely the pre-S1(9-15) region responsible for essential NTCP binding [18], the pre-S1(9-24) region responsible for heparin binding and membrane disruption/fusion, and the pre-S1(30-42) for heparin binding (see Fig. 18). So far, it has been considered that HBV initially interacts with receptor HSPG and then moves to NTCP, both events occurred on the cell surface [18]. From my results, both pre-S1(9-24) and pre-S1(30-42) are involved in the initial attachment of HBV with highly sulfated GAGs of HSPG on the surface of human hepatic cells. Since HSPGs consist of a core protein associated with various GAG chains, the heparan sulfate GAG diversity found in HSPGs (i.e., N- and O-sulfation and epimerizations [19]) could contribute to different biological functions of them [20]. One research group previously found that almost all syndecan and glypican families (members of HSPGs) are involved in the cell entry of HBV, whereas agrin and perlecan not. Especially, glypican 5 is the most responsible to the cell attachment and entry of HBV among HSPGs [21]. Actually, high concentration of heparin (i.e., 10-100 μg/mL) could block the HBV infection completely *in vitro* [22]. Meanwhile, another research group demonstrated that physiological concentration of heparin could enhance the HBV infection to human hepatic cells in a pre-S1 region- and NTCP-dependent manner. Especially, O-sulfation of heparin is more efficient for the enhancement of HBV infection than N-sulfation of heparin [23]. In future, it would be necessary for clarifying the aforementioned discrepancies in the role of HSPGs to elucidate how the evolutionally conserved residues Asp-31, Trp-32, and Asp-33 of pre-S1(30-42) interact with GAGs on the molecular basis. Moreover, I speculate that the interaction with highly sulfated GAGs

could trigger the conformational change of pre-S1 region (i.e., pre-S1(9-15)) for NTCP binding in the endosomes. The NTCP interaction may change the conformation of pre-S1(9-24) fusogenic domain, leading to the membrane interaction.

HSPG is an endocytosis receptor, which plays a pivotal role in the initial interaction and cell entry of a large number of DDS nanocarriers [24-26]. Generally, these nanocarriers, for examples cell penetrating peptide-modified LPs and heparin binding peptide-modified LPs, charged positively, which could interact with negatively charged HSPG through electrostatic interaction. However, these nanocarriers are often phagocyted by macrophages *in vivo* more efficiently than negatively charged nanocarriers, resulting in undesired biodistribution, such as the accumulation in lung, liver, and spleen [27, 28]. As described in Chapter III, the pre-S1(30-42)-displaying LPs exhibited stronger heparin-binding activity and hepatotropic property than the LPs displaying conventional positively charged heparin-binding peptides. Thus, negatively charged pre-S1(30-42) is more ideal targeting molecule for the forthcoming HSPG-targeting DDS nanocarriers. Comparing with other HBV-mimicking DDS nanocarriers, such as pre-S1 peptide-modified micelles and nanocages, the pre-S1(30-42)-displaying LPs possess the following advantages: 1) the enveloped structure of LPs is very similar to that of HBV, being suitable for displaying the HBV-derived functional domains indispensable for the early infection machinery; 2) LP-based DDS nanocarriers have been already demonstrated as the most successful platform for clinical use [29]; 3) pre-S1(30-42) exhibits the highest HSPG-interacting activity and shortest structure among HBV-derived HSPG-interacting peptides, which is very useful for DDS nanocarriers; 4) pre-S1(30-42) exhibits higher hepatotropic property than other pre-S1-derived peptides; 5) pre-S1(30-42) can induce endocytosis more efficiently than other pre-S1-derived peptides. In near

future, the combination of pre-S1(30-42) and pre-S1(9-24) would facilitate the development of ideal HBV-mimicking DDS nanocarriers harboring complete HBV early infection machinery (i.e., HSPG-mediated cell attachment, cell entry by endocytosis, transfer to NTCP in endosomes, disruption/fusion of endosomal membrane and nanocarrier's membrane, and cytoplasmic release of payloads by endosomal escape).

References

1. T.M. Allen, P.R. Cullis, Drug delivery systems: entering the mainstream, *Science*, 2004, 303, 1818-1822.
2. A.Z. Wilczewska, K. Niemirowicz, K.H. Markiewicz, H. Car, Nanoparticles as drug delivery systems, *Pharmacological Reports*, 2012, 64, 1020-1037.
3. G. Tiwari, R. Tiwari, B. Sriwastawa, L. Bhati, S. Pandey, P. Pandey, S.K. Bannerjee, Drug delivery systems: an updated review, *International Journal of Pharmaceutical Investigation*, 2012, 2, 2-11.
4. S. Wilhelm, A.J. Tavares, Q. Dai, S. Ohta, J. Audet, H. F. Dvorak, W. C. W. Chan, Analysis of nanoparticle delivery to tumours, *Nature Reviews Materials*, 2016, 1, 1–12.
5. H. Yin, R.L. Kanasty, A.A. Eltoukhy, A.J. Vegas, J.R. Dorkin, D.G. Anderson, Non-viral vectors for gene-based therapy, *Nature Reviews Genetics*, 2014, 15, 541-555.
6. M. Somiya, Q. Liu, S. Kuroda, Current progress of virus-mimicking nanocarriers for drug delivery, *Nanotheranostics*, 2017, 1, 415-429.
7. S. Kuroda, S. Otaka, T.Miyazaki, M. Nakao, Y. Fujisawa, Hepatitis B virus envelope L protein particles: synthesis and assembly in Saccharomyces cerevisiae, purification and characterization, *Journal of Biological Chemistry*, 1992, 267, 1953–1961.

8. T. Yamada, Y. Iwasaki, H. Tada, H. Iwabuki, M.K. Chuah, T. Vanden, Driessche, H. Fukuda, A. Kondo, M. Ueda, M. Seno, K. Tanizawa, S. Kuroda, Nanoparticles for the delivery of genes and drugs to human hepatocytes, *Nature Biotechnology*, 2003, 21, 885-890.
9. J. Jung, T. Matsuzaki, K. Tatematsu, T. Okajima, K. Tanizawa, S. Kuroda, Bio-nanocapsule conjugated with liposomes for in vivo pinpoint delivery of various materials, *Journal of Controlled Release*, 2008, 126, 255-264.
10. T. Kasuya, J. Jung, R. Kinoshita, Y. Goh, T. Matsuzaki, M. Iijima, N. Yoshimoto, K. Tanizawa, S. Kuroda, Bio-nanocapsule–liposome conjugates for in vivo pinpoint drug and gene delivery, *Methods in Enzymology*, 2009, 464, 147-166.
11. Q. Liu, J. Jung, M. Somiya, M. Iijima, N. Yoshimoto, T. Niimi, A.D. Maturana, S.H. Shin, S.Y. Jeong, E.K. Choi, S. Kuroda, Virosomes of hepatitis B virus envelope L proteins containing doxorubicin: synergistic enhancement of human liver-specific antitumor growth activity by radiotherapy, *International Journal of Nanomedicine*, 2015, 10, 4159-4172.
12. J. Jung, M. Somiya, S.Y. Jeong, E.K. Choi, S. Kuroda, Low immunogenic bio-nanocapsule based on hepatitis B virus escape mutants, *Nanomedicine*, 2018, 14, 595-600.
13. F. Madani, S. Lindberg, U. Langel, S. Futaki, A. Gräslund, Mechanisms of cellular uptake of cell-penetrating peptides, *Biophysical Journal*, 2011, 2011, 414729.
14. A. Ziegler, Thermodynamic studies and binding mechanisms of cell-penetrating peptides with lipids and glycosaminoglycans, *Advanced Drug Delivery Reviews*, 2008, 60, 580-597.

15. A.K. Varkouhi, M. Scholte, G. Storm, H.J. Haisma, Endosomal escape pathways for delivery of biologicals, *Journal of Controlled Release*, 2011, 151, 220-228.
16. X. Han, J.H. Bushweller, D.S. Cafiso, L.K. Tamm, Membrane structure and fusion-triggering conformational change of the fusion domain from influenza hemagglutinin, *Nature Structural & Molecular Biology*, 2001, 8, 715-720.
17. Y.S. Mendes, N.S. Alves, T.L. Souza, I.P. Sousa, Jr., M.L. Bianconi, R.C. Bernardi, P.G. Pascutti, J.L. Silva, A.M. Gomes, A.C. Oliveira, The structural dynamics of the flavivirus fusion peptide-membrane interaction, *PLoS One*, 2012, 7, e47596.
18. S. Urban, R. Bartenschlager, R. Kubitz, F. Zoulim, Strategies to inhibit entry of HBV and HDV into hepatocytes, *Gastroenterology*, 2014, 147, 48-64.
19. C.M. Leistner, S. Gruen-Bernhard, D. Glebe, Role of glycosaminoglycans for binding and infection of hepatitis B virus, *Cellular Microbiology*, 2008, 10, 122-133.
20. S. Sarrazin, W. C. Lamanna, J.D. Esko, Heparan Sulfate Proteoglycans, *Cold Spring Harbor Perspectives in Biology*, 2011, 3, a004952.
21. E.R. Verrier, C.C. Colpitts, C. Bach, L. Heydmann, A. Weiss, M. Renaud, S.C. Durand, F. Habersetzer, D. Durantel, G. Abou-Jaoudé, M.M. López Ledesma D.J. Felmlee, M. Soumillon, T. Croonenborghs, N. Pochet, M. Nassal, C. Schuster, L. Brino, C. Sureau, M.B. Zeisel, T.F. Baumert, A targeted functional RNA interference screen uncovers glypican 5 as an entry factor for hepatitis B and D viruses, *Hepatology*, 2016, 63, 35-48.
22. A. Schulze, P. Gripon, S. Urban, Hepatitis B virus infection initiates with a large surface protein-dependent binding to heparan sulfate proteoglycans, *Hepatology*, 2007, 46, 1759-1768.

23. G. Choijilsuren, R.S. Jhou, S.F. Chou, C.J. Chang, H.I. Yang, Y.Y. Chen, W.L. Chuang, M.L. Yu, C. Shih, Heparin at physiological concentration can enhance PEG-free in vitro infection with human hepatitis B virus, *Scientific Reports*, 2017, 7, 14461.
24. Helena C. Christianson, Katrin J. Svensson, Toin H. van Kuppevelt, Jin-Ping Li, and Mattias Belting, Cancer cell exosomes depend on cell-surface heparin sulfate proteoglycans for their internalization and functional activity, *Proceedings of the National Academy of Sciences of the United States of America*, 2013, 110, 17380-17385.
25. I. Sauer, I.R. Dunay, K. Weisgraber, M. Bienert, M. Dathe, An apolipoprotein E-derived peptide mediates uptake of sterically stabilized liposomes into brain capillary endothelial cells, *Biochemistry*, 2015, 44, 2021-2029.
26. C. Marty, C. Meylan, H. Schott, K. Ballmer-Hofer, R.A. Schwendener, Enhanced heparan sulfate proteoglycan-mediated uptake of cell-penetrating peptide-modified liposomes, *Cellular and Molecular Life Sciences*, 2004, 61, 1785-1794.
27. C. He, Y. Hu, L. Yin, C. Tang, C. Yin, Effects of particle size and surface charge on cellular uptake and biodistribution of polymeric nanoparticles, *Biomaterials*, 2010, 31, 3657-3666.
28. Y. Tabata, Y Ikada. Effect of the size and surface charge of polymer microspheres on their phagocytosis by macrophage. *Biomaterials*, 1988, 9, 256-362.
29. V.J. Venditto, F.C. Szoka Jr, Cancer nanomedicines: so many papers and so few drugs!, *Advanced Drug Delivery Reviews*, 2013, 65, 80-88.

Acknowledgements

This study has been performed at the Institute of Scientific and Industrial Research, Osaka University from 2016 to 2019 under the direction of Prof. Shun'ichi Kuroda in the Department of Biomolecular Science and Reaction. During this study, I received financial assistance from Japan Society for the Promotion of Science as fellowships DC2, and the Institute of Scientific and Industrial Research, Osaka university as research assistant.

I also received kindly helps from many people during this study. First of all, I deeply appreciate to Prof. Shun'ichi Kuroda at Osaka University for his support, encouragement and helpful discussions. I would like to thank Profs. Masaharu Somiya, Kenji Tatematsu, Toshihide Okajima, Masumi Iijima, Tadashi Nakai, Nobuo Yoshimoto for their kindly comments and supports. I also thank the member of Department of Biomolecular Science and Reaction during this study. Furthermore, I am very grateful to my parents and girlfriend for their encouragement and mental supports. At last, I would like to thank all the people who participated in this study.

List of Publications

Original papers

1. Q. Liu, J. Jung, M. Somiya, M. Iijima, N. Yoshimoto, T. Niimi, A.D. Maturana, S.H. Shin, S.Y. Jeong, E.K. Choi, S. Kuroda, Virosomes of hepatitis B virus envelope L proteins containing doxorubicin: synergistic enhancement of human liver-specific antitumor growth activity by radiotherapy, *International Journal of Nanomedicine,* 2015, 10, 4159-4172.
2. M. Somiya, K. Yamaguchi, Q. Liu, T. Niimi, A.D. Maturana, M. Iijima, N. Yoshimoto, S. Kuroda, One-step scalable preparation method for non-cationic liposomes with high siRNA content, *International Journal of Pharmaceutics*, 2015, 490, 316–323.
3. M. Somiya, Y. Sasaki, T. Matsuzaki, Q. Liu, M. Iijima, N. Yoshimoto, T. Niimi, A.D. Maturana, S. Kuroda, Intracellular trafficking of bio-nanocapsule-liposome complex: Identification of fusogenic activity in the pre-S1 region of hepatitis B virus surface antigen L protein, *Journal of Controlled Release*, 2015, 212, 10-18.
4. Q. Liu, M. Somiya, N. Shimada, W. Sakamoto, N. Yoshimoto, M. Iijima, K. Tatematsu, T. Nakai, T. Okajima, A. Maruyama, S. Kuroda, Mutational analysis of hepatitis B virus pre-S1 (9-24) fusogenic peptide, *Biochemical and Biophysical Research Communications,* 2016, 474, 406-412. (Chapter II of this thesis)
5. M. Somiya, Q. Liu, N. Yoshimoto, M. Iijima, K. Tatematsu, T. Nakai, T. Okajima, K. Kuroki, K. Ueda, S. Kuroda, Cellular uptake of hepatitis B virus envelope L particles is independent of sodium taurocholate cotransporting polypeptide, but dependent on heparan sulfate proteoglycan, *Virology*, 2016, 497, 23-32.
6. H. Li, K. Onbe, Q. Liu, M. Iijima, K. Tatematsu, M. Seno, H. Tada, S. Kuroda, Synthesis and assembly of hepatitis B virus envelope protein-derived particles in

Escherichia coli, *Biochemical and Biophysical Research Communications*, 2017, 490, 155-160.

7. Q. Liu, M. Somiya, M. Iijima, K. Tatematsu, S. Kuroda, A hepatitis B virus-derived human hepatic cell-specific heparin-binding peptide: Identification and application to a drug delivery system, *Biomaterials Science*, 2019,7, 322-335. (Chapter III of this thesis)
8. M. Iijima, K. Araki, Q. Liu, M. Somiya, S. Kuroda, Oriented immobilization to nanoparticles enhanced the therapeutic efficacy of antibody drugs, *Acta Biomaterialia*, 2019, 86, 373-380.

Review papers

1. Q. Liu, M. Somiya, S. Kuroda, Elucidation of the early infection machinery of hepatitis B virus by using bio-nanocapsule, *World Journal of Gastroenterology,* 2016, 22, 8489-8496.
2. M. Somiya*, Q. Liu*, S. Kuroda, Current progress of virus-mimicking nanocarriers for drug delivery, *Nanotheranostics*, 2017, 4, 415-429. (*These authors contributed equally to this work)

International and Domestic Meetings, and Awards

Presentations in international conferences

1. Q. Liu, M. Somiya, S. Kuroda, Possible involvement of HBV pre-S1 (9-24) fusogenic peptide in uncoating process, 2016 International HBV Meeting, Seoul, Korea, Sep. 21-24, 2016 (Poster).
2. Q. Liu, M. Somiya, S. Kuroda, Elucidation of early infection machinery of hepatitis B virus and bio-nanocapsule, The 20th SANKEN International The 15th SANKEN Nanotechnology Symposium, Osaka, Japan, Dec. 12-13, 2016 (Poster).
3. Q. Liu, M. Somiya, S. Kuroda, Analysis of cell attachment and entry of hepatitis B virus, 5th JAPAN-TAIWAN-KOREA HBV Research Symposium 2017, Apr. 8-9, 2017, Tokyo, Japan (Oral).
4. Q. Liu, M. Somiya, S. Kuroda, Novel heparin-binding domain of hepatitis B virus: Application to drug delivery system, Biomaterials International 2017, Aug. 20-24, 2017, Fukuoka, Japan (Oral).
5. Q. Liu, M. Somiya, S. Kuroda, Creation and application of hepatitis B virus-mimicking nanoparticle for drug delivery, The 21st SANKEN International Symposium, Jan. 16-17, 2018, Osaka, Japan (Poster).
6. Q. Liu, M. Somiya, S. Kuroda, Identification of hepatitis B virus-derived heparin-binding domain: application for liposomal drug delivery, 2018 CRS Annual Meeting and Exposition, Jul. 22-24, 2018, New York, U.S.A (Poster).

Presentations in domestic meetings

1. Q. Liu, T. Nakamoto, M. Somiya, M. Iijima, S. Kuroda, バイオナノカプセル-リポソーム複合体による抗がん剤(ドキソルビシン)のヒト肝臓由来組織への能動的送達, The 30th Annual Meeting of the Japan Society of Drug Delivery System, Jul. 30-31, 2014, Tokyo, Japan (Oral).
2. Q. Liu, S. Kuroda, B 型肝炎ウイルス外皮 L タンパク質由来 Virosome の創製及び DDS への応用、日本農芸化学会関西支部例会 第 492 回講演会, Dec. 5, 2015, Kobe, Japan (Oral).
3. Q. Liu, M. Somiya, S. Kuroda, B 型肝炎ウイルス外皮 L タンパク質由来 Virosomes の創製及び同ドキソルビシン封入体の抗がん活性, The 67th Annual Meeting of the Society for Biotechnology, Oct. 26-28, 2016, Kagoshima, Japan (Poster).
4. Q. Liu, M. Somiya, S. Kuroda, 合成ペプチドを用いてバイオナノカプセルのエンドソーム脱出メカニズムの解析, The 32nd Annual Meeting of the Japan Society of Drug delivery system, Jun. 30-Jul. 1, 2016, Shizuoka, Japan (Oral).
5. Q. Liu, M. Somiya, S. Kuroda, B 型肝炎ウイルス及びバイオナノカプセルの初期感染機構の解析, The 68th Annual Meeting of the Society for Biotechnology, Sep. 28-30, 2016, Toyama, Japan (Poster).

6. Q. Liu, M. Somiya, S. Kuroda, B 型肝炎ウイルスの新規細胞結合ドメインの同定及び受容体の探索, 日本生物工学会セルプロセッシング計測評価研究部会第９回若手研究シンポジウム, Jul. 22, 2017, Hiroshima, Japan (Oral).

7. Q. Liu, M. Somiya, S. Kuroda, B 型肝炎ウイルスの新規細胞結合ドメインの同定, 日本生物工学会 2017 年度生物工学若手研究者の集い（若手会）, Jul. 21-22, 2017, Hiroshima, Japan (Poster).

8. Q. Liu, M. Somiya, S. Kuroda, B 型肝炎ウイルスの新規細胞接着ドメインの同定及び DDS への応用, The 69th Annual Meeting of the Society for Biotechnology, Sep. 11-14, 2017, Tokyo, Japan (Poster).

9. Q. Liu, M. Somiya, S. Kuroda, B 型肝炎ウイルス由来の新規ヘパリン結合ドメインの同定及び DDS への応用, The 34nd Annual Meeting of the Japan Society of Drug Delivery System, Jun. 21-22, Nagasaki, Japan (Oral).

Awards

公益社団法人日本生物工学会第 5 回生物工学学生優秀賞（飛翔賞）, Japan, 2016.